Sonochemical Fixation of Nitrogen

By

Supeno

A Thesis submitted to the
Faculty of Graduate Studies and Research
In partial fulfillment of the
Requirement for the degree of

Master of Science

Department of Chemistry

Carleton University
Ottawa, Ontario
June, 2000

Abstract

The production of nitrogen fertilizer requires ammonia. It is synthesized industrially by the "Haber-Bosch"process, where conditions are extreme, e.g. 200 atm and 650 K. Such conditions are found in the collapse of cavitation bubbles formed when a liquid is exposed to high-intensity ultrasound. The eventual aim of this research is to see if ultrasonic irradiation of liquids saturated with N_2 and other appropriate gases can result in sufficiently effective nitrogen fixation to have commercial applications. This is why the experiments were extended to ammonia formation in alkanes with N_2/H_2 mixtures. Such sonication systems could be used with a catalyst to increase the rate of ammonia production.

The formation of nitrite (NO_2^-) and nitrate (NO_3^-) was observed in water with a gaseous N_2/O_2 mixture bubbled through it while being exposed to 900 kHz ultrasound intense enough to cause cavitation. The formation of NO_x^- (total nitrite and nitrate) was followed both by pH and nitrate ion specific electrodes. The maximum rate (30 nmol min^{-1} W^{-1}) was observed when the gas mixture had 0.6 mol fraction N_2. This is in reasonable agreement with the results of other studies. No formation of NO_x^- was observed in the absence of O_2 gas, i.e. the oxygen for NO_x can not be obtained from water.

Ammonia (NH_3) can be obtained when a gaseous mixture of N_2 and H_2 is bubbled through water. The maximum rate of formation occurs with 0.6 mol fraction N_2 gas. Detection of ammonia (as ammonium ion) is possible through pH, but the use of Nessler's reagent and UV-visible absorption is more reliable. In this case some ammonia is detected with no hydrogen gas; some hydrogen must be available from the sonochemical dissociation of water.

Ammonia is also formed when N_2/H_2 gas mixtures are bubbled through an alkane which is irradiated by ultrasound. The rate decreases with increasing bulk temperature, suggesting that kinetic, rather than thermodynamic, considerations predominate. The presence of some standard Haber-Bosch ammonia catalyst in the region of cavitational activity (in octane) did not increase the rate of ammonia formation.

Acknowledgements

I would like to take this opportunity to express my deepest appreciation and many tanks to all people who directly and indirectly contributed to my graduate career.

First and foremost I would like to acknowledge my thesis supervisor Professor Peeter Kruus for his kindness, guidance, patience and ideas throughout this research work. He has also opened my blindness from scientific method, writing and creativity.

Dr. Donald R. Wiles, for his inspiration to welcome at Carleton University and his special friendship.

Dr. Robert Burk at Center for the Analytical and Environmental Chemistry for the important help on GC-MS.

Mr. Fred Cassalman and Mr. Tony O'niel, for their much helpful guidance on instrumentations.

Mr. Robert Kehle and Mr. Keith Bourque at the chemistry store room for all their help with purchasing chemicals.

Mr. John Murimboh and Ms. Rocio Aranda, for their help with computer and preliminary laboratory.

Haldor-Topsoe, Denmark, for the catalyst.

East Indonesian Universities Development Project for the financial support.

Finally, I would like to thank my family for their patience, support and undivided love.

Publications and Presentations

The following publication and presentations have resulted from this work:

Refereed Contribution

Supeno; Kruus, P. "Sonochemical Formation of Nitrate and Nitrite in Water", Not be issued yet by Ultrasonics Sonochemistry.

Non-Refereed Contributions

Supeno; Kruus, P. "Sonochemical Fixation of Nitrogen", OCCI day, Poster Presentation, May 2000, Ottawa, Canada.

Supeno; Kruus, P. "Sonochemical Fixation of Nitrogen in Water", 7th Meeting of the European Society of Sonochemistry, Poster Presentation, May 2000, Biarritz-Guethary, France.

Supeno; Kruus, P. "Sonochemical Fixation of Nitrogen" The 83rd Canadian Society for Chemistry Conference, Poster Presentation, May 2000, Calgary, Canada.

Table of Contents

List of Figures

List of Tables

Introduction

1.1. Cavitation

The term cavitation refers to the formation, growth and violent collapse of bubbles in liquids [Webster, 1963]. This bubble can be either gas or vapour, present in any liquid such as water, organic solvent or molten metal under a wide range of conditions.

Sir John Thornycroft in 1895 first used the term of "cavitation" in his observation for erosion on the propellers of torpedo boat destroyers. In 1917, Lord Rayleigh investigated this mechanical cavitation problem and confirmed that the vibrations were caused by the enormous turbulence, heat and pressure of imploding cavities.

There are at least three stages of acoustic cavitation [Suslick, 1990]: nucleation, bubble growth and implosive collapse. Nucleation of bubbles is difficult in a pure liquid due to its high tensile strength. Theoretical estimation of tensile strength of a pure liquid varies from (– 500 atm) to (– 10,000 atm) [Frenkel, 1948]. This means that a liquid should not rupture and form the nucleus for a cavity until such a negative pressure is applied to it.

Pure water has a theoretical tensile strength of order of (-1000 atm). The tensile strength of pure water obtained experimentally is less; even for extremely clean water, it is only (-300 atm) [Kuttruff, 1991]. This is because even in the cleanest possible water there will be some defects, e.g. those caused by cosmic radiation.

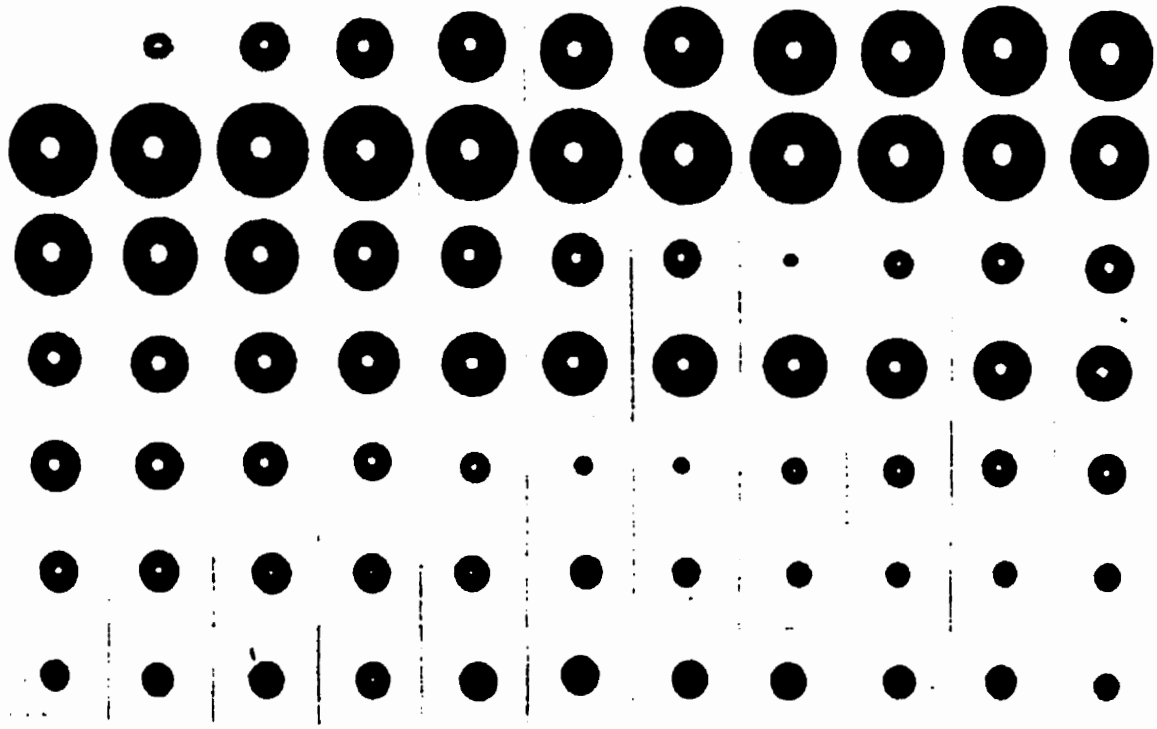

Figure 1.1.1: High-speed cinematographic pictures of spherical cavitation bubble far from boundaries, imploding cavity in silicon oil (Lauterbon, 1973).

The origin of cavitation can be hydrodynamic, thermal or acoustic. In sonication, cavitation will occur when the pressure amplitude of the applied sound reaches a certain minimum called the cavitation threshold. Galloway [1954] found that the cavitation threshold decreases with increasing amount of air in a liquid. The air bubbles act as nuclei for formation of cavitation.

Acoustic cavitation is generally classified into two types: transient and stable [Suslick, 1988]. Transient cavitation has a large variation in the bubble radius relative to its equilibrium size, and lasts over a time of a few acoustic cycles. The cavity grows rapidly and usually terminates in a collapse of varying degrees of violence.

Stable cavitation, on the other hand, usually has a bubble size approaching a resonant radius. The bubble grows slowly over many acoustic cycles. Suslick [1990] reported on dependence of the resonant size on frequency. For a frequency $\nu = 20$ kHz, the resonant size of radius R_o for air bubbles in water approaches 85 μm. The relationship between bubble radius and frequency of the applied sound wave for the simple radial oscillator is given below [Smith, 1935]:

$$\nu = [1/(2\pi R)] / [\, 3\gamma(P^o + 2\sigma/R)/\rho]^{1/2} \qquad (1.1.1)$$

Which may be written [Hueter, 1955]:

$$R_o = 1/\omega[3\gamma P^o/\rho]^{1/2} \approx 326\, P^{o\,1/2}/\nu \text{ (cm)}, \qquad \text{if } Po >> 2\sigma/R \qquad (1.1.2)$$

And by:

$$R_o = 1/\omega[6\gamma\sigma/\rho R_o]^{1/2} \approx (3.9/\nu)^{1/2} \text{ (cm)}, \qquad \text{if } Po << 2\sigma/R \qquad (1.1.3)$$

Here, ν is the frequency of the applied sound wave, R the radius of the bubble, γ the ratio of the specific heats of the gas in the bubble, P^o the external hydrostatic pressure, σ

the surface tension of the liquid/gas interface, ρ the density of the liquid, and ω the radial frequency of the ultrasound ($=2\pi\nu$).

When bubbles collapse, they produce an extreme condition called a "hot spot". The temperature reaches thousands of degrees [Fitzgerald, 1954; Suslick, 1990; Didenko, 1999]. Suslick et al. 1990 estimated a temperature in the order of 5000 K and pressure in the order of 500 atm.

The hot-spot temperature is also dependent on the vapour pressure of liquid. This can be shown from experimental results by Didenko, 1999 and Flint, 1991. They found the temperature to be 4300 ± 200 K, at 6.6 torr, in a water – benzene mixture, and 5080 ± 160 K, at < 0.01 torr, in silicon oil. This condition is sufficiently extreme to cause chemical reactions.

The primary chemical reactions are the fragmentation of solvent and volatile solute vapour in the hot spots to yield more simple compounds or radical species [Currell, 1958; Anbar, 1964; Hart et al., 1990]. In the sonication of water, the primary reaction produces reactive species such as $H^{\bullet}$, $OH^{\bullet}$ and H_2O_2. These can lead to a secondary reaction such as oxidation of iodide to iodine [Entezari and Kruus, 1994].

In 1955, Lindstrom proposed the mechanism of primary reaction in water sonolysis. Around three decades later, Reisz et al. [1985] had demonstrated through spin trapping experiments that sonication in water produces $OH^{\bullet}$ and $H^{\bullet}$ radicals from the thermal decomposition of water vapour contained inside the cavitation bubbles. Other investigation of $OH^{\bullet}$ concentration obtained during sonication can be found in several articles [Mason et al. 1994; Renaudin et al. 1994; Petrier et al., 1999].

The primary and secondary reactions are summarized as below:

$$H_2O \rightarrow H^{\bullet} + OH^{\bullet} \qquad (1.1.4)$$

$$H^{\bullet} + H^{\bullet} \rightarrow H_2 \qquad (1.1.5)$$

$$OH^{\bullet} + OH^{\bullet} \rightarrow H_2O_2 \qquad (1.1.6)$$

In the presence of air, the secondary reaction was postulated as below [Weissler, 1959; Margulis, 1984; Hart, 1985], where O_2 molecules from air can act as a scavenger for H:

$$H^{\bullet} + O_2 \rightarrow OOH^{\bullet} \qquad (1.1.7)$$

Another radical reaction can occur:

$$OOH^{\bullet} + OH^{\bullet} \rightarrow H_2O + O_2 \qquad (1.1.8)$$

In the presence of iodide (e.g. 0.20 M KI solution), the overall reaction is:

$$2OH^{\bullet} + 3I^{-} \rightarrow 2OH^{-} + I_3^{-} \qquad (1.1.9)$$

Since I_3^- absorbs strongly at 355 nm, this reaction is often used to calibrate the intensity of cavitation (see appendix E.1). It is commonly called the "Weissler reaction" [Weissler, 1950]

There is a frequency dependence for the rate of sonochemical reactions. Tiehm [1999] found a frequency dependence in his research of biodegradation of polycyclic aromatic hydrocarbons under ultrasonic treatment. In a frequency range from 41 kHz to 3.2 MHz, he found the maximum rate of production of nitrate to occur at 360 kHz. The dependence of reaction rate on frequency is presumably due to the variation of the resonant radius of cavitation bubbles with frequency, as well as the effectiveness of producing cavitation with frequency (at constant acoustic power).

1.2. Nitrogen Fixation

More food is required to feed the steadily increasing world population. Plants for food require nitrogen to grow. There is plenty of nitrogen gas in the atmosphere, but most food plants are unable to consume nitrogen directly from the air. They usually obtain it in the form of compounds such as nitrite, nitrate and ammonia present in the soil. Therefore more research should be done to synthesize such compounds industrially for fertilizers.

Ammonia production is now second only to sulphuric acid in terms of mass produced. In 1996-1997, the world consumption of fertilizers reached 134.4 million tons of nutrients. Of this, 82.5 million tons was N, 20.8 million tons K_2O and 31.1 million tons P_2O_5 [Faust, 1999].

Ammonia is the primary material in the manufacture of agricultural fertilizers. In the early 1900s, chemists were challenged to synthesize ammonia from available raw materials. This was eventually achieved by Fritz Haber, professor of chemistry at Karlsruhe in Germany, in 1907. He succeeded in synthesizing ammonia catalytically from its elements at high temperature and pressure. Karl Bosch in 1913 then optimized this process by providing the suitable engineering conditions. In that time, about 7000 tons of ammonia were being produced. The overall reaction of ammonia formation is the following:

$$N_{2(g)} + 3\,H_{2(g)} = 2\,NH_{3(g)} \qquad (1.2.1)$$

There is no reaction for reactants at ambient temperature, or even close to 1000°C. This is due to unfavourable kinetics. Only above 3000°C does the reaction occur

significantly without catalyst. At that temperature, most of H_2 and N_2 are dissociated to H and N atoms, which then form ammonia [Twigg, 1996].

This condition, however, is thermodynamically not favourable for formation of ammonia; it is favoured thermodynamically at lower temperatures. A catalyst is thus required to compromise the thermodynamic and kinetic problems in ammonia production. Ammonia can be produced in significant amounts with a catalyst at 400°C and 200 atmospheres.

In nature, the most important nitrogen-fixing species are the mutualistic species of Rhizobium living in root nodules of various species of legumes such as clover, alfalfa, beans, and peas [Huheey, 1978]. Complex enzymatic processes with anaerobic conditions produce ammonia.

In aquatic or marine environments, ammonia production is through an ammonication process [Libes, 1992]. When dissolved organic nitrogen is formed in seawater, heterotrophic bacteria degrade it. This degradation is rapid due to the relatively high reactivity of the carbon-nitrogen bonds. The complete degradation releases ammonia (NH_3), which reacts with H^+ or H_2O to form ammonium (NH_4^+). This process is called ammonification.

The presence of the bacteria nitrosomonas and nitrobacter in seawater will lower the ammonia concentration. Bacteria nitrosomonas oxidizes NH_4^+ to produce nitrite. This product is then converted to nitrate by nitrobacter. This process is called nitrification.

The ammonification and nitrification processes are illustrated below:

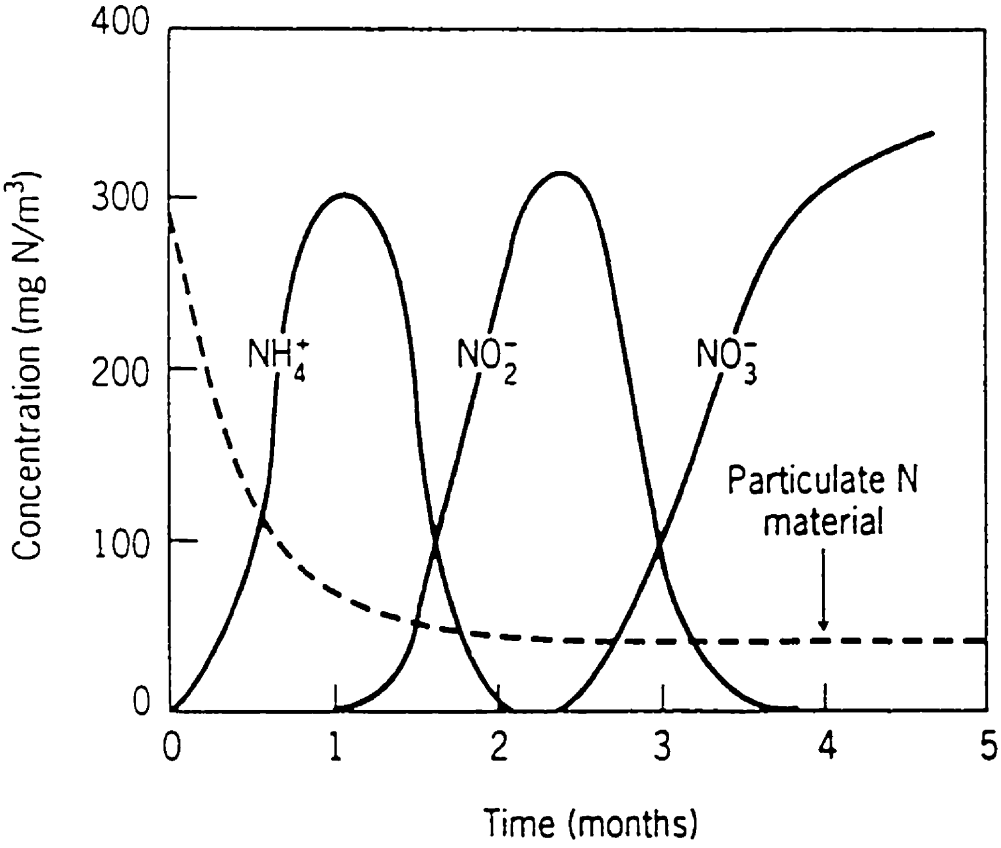

Figure 1.2.1: Production of nitrogeneous compounds from decomposition of phytoplankton in aerated water stored in the dark, after Horne, 1979 as presented in Libes, 1992.

1.3. Review of Previous Work

1.3.1. Sonochemical Formation of Nitrite and Nitrate

Sonochemical formation of nitrite and nitrate in water was noted as far back as 1936 by Schultes and Gohr. After irradiation with 540 kHz ultrasound, the acidity of the water had increased and chemical tests showed the presence of nitrite.

In 1950, Virtanen and Ellfolk reported on the pH dependence of the formation nitrite and nitrate in aqueous solution. The rate of formation of total nitrite plus nitrate ($r_{NO_x^-}$) was roughly independent of pH, but the ratio of nitrate to nitrite increased considerably as the pH decreased. They used 300 kHz ultrasound at 10 W cm^{-2} (130 W total) in their experiments.

Mead et al. in 1976 determined that the initial rates of nitrite and nitrate formation in water saturated with air were 22. x 10^{-6} and 6. x 10^{-6} M min^{-1}, respectively. They used 447 kHz ultrasound at 50 W irradiating 50 mL water samples at 298 K.

Recently, Tiehm [1999] has investigated the dependence of nitrite and nitrate formation in air-saturated water as a function of ultrasonic frequency from 41 to 3217 kHz. The maximum production occurs at 360 kHz; the rates at 41 and 1068 kHz are about 60% of this maximum rate. When 250 mL of water at 298 K was irradiated with 50 W of 360 kHz ultrasound over one hour, the production of nitrate was 7.1 mg L^{-1}, and of nitrite 0.6 mg L^{-1}. This corresponds to a rate of formation of nitrate and nitrite of 13. x 10^{-9} and 1. x 10^{-9} mol min^{-1} W^{-1}, respectively.

In the same publication, Petrier et al. [1999] reported on the formation of nitrate, nitrite and hydrogen peroxide in 200 mL of air-saturated water at 293 K with 30 W of

500 kHz ultrasound over a five-hour period. The concentration of nitrate increased steadily, while nitrite decreased after 100 min of ultrasonic irradiation. The rate of hydrogen peroxide formation was initially about the same as the total nitrate plus nitrite, but decreased after 100 min. Petrier et al. suggested that nitrite and hydrogen peroxide are the primary products, and nitrate results from the oxidation of nitrite by hydrogen peroxide through a reaction whose rate is dependent on pH. The rate of total nitrate plus nitrite formation was 33. x 10^{-9} mol min^{-1} W^{-1}.

In another recent paper [Wakeford et al., 1999], the dependence of the rate of nitrite production with ionic strength was investigated. In air-saturated aqueous salt solutions, the rate increased from 0.3 x 10^{-6} M min^{-1} at zero ionic strength to as high as 1.8 x 10^{-6} M min^{-1} W^{-1} in a solution of sodium sulphate with ionic strength 2.5 mol L^{-1}. These studies were done with 35 kHz ultrasound with samples of 659 mL at 293 K. No power data were provided.

There have been suggestions that the oxygen required for NO_x formation comes from the decomposition of oxygen molecules (O_2) in the imploding cavities [Wakeford et al., 1999], rather than from decomposition of water. There is good evidence that dissociation of O_2 occurs in cavitation [Fischer, 1986]. The possibility of the dissociation of nitrogen molecules [Sokol'skaya, 1978] in the cavities has also been suggested.

The NO_x formation can be of significance in nature, as hydrodynamic cavitation occurs in breaking waves and waterfalls [Anbar, 1968], and there is now good evidence that hydrodynamic cavitation has some of the properties of cavitation produced by intense ultrasound [Morita, 1966; Suslick, 1997]. The process is also related to the

formation of NO_x in internal combustion engines [Heywood, 1988], and to the formation of acid rain from dissolution of gaseous NO_x [Seinfeld, 1998].

1.3.2. Sonochemical Formation of Ammonia

In 1957, El'piner and Sokol'skaya reported the sonochemical formation of ammonia from its elements. They irradiated the water containing hydrogen, nitrogen only and a mixture of both gases in hermitically sealed glass vessels as a function of time with 380 kHz ultrasound (6-7 W cm^{-2}).

They found that with N_2 alone, 0.62 μg/mL of ammonia had formed after 120 minutes. With a mixture of N_2 and H_2 present, the ammonia concentration reached 2.6 μg/mL after 120 minutes and 12.5 μg/mL after 360 minutes irradiation. There is no information for the gas composition of nitrogen and hydrogen used in this research.

It is believed that the ultrasonic irradiation of hydrogen and nitrogen gases in the solution produce hydrogen and nitrogen atoms which then formed ammonia [Sokol'skaya, 1978].

$$H_2 \rightarrow H^\bullet + H^\bullet \qquad (1.3.2.1)$$

$$N_2 \rightarrow N^\bullet + N^\bullet \qquad (1.3.2.2)$$

$$N^\bullet + H^\bullet \rightarrow NH \qquad (1.3.2.3)$$

$$NH + H_2 \rightarrow NH_3 \qquad (1.3.2.4)$$

In 1986 Fisher et al. reported ultrasonic dissociation of hydrogen gases. Water containing a mixture of argon and HD was irradiated by 300 kHz of ultrasound for 30 minutes. They found that H_2 and D_2 formed. The maximum rate of H_2 formation was obtained for 50 volume % HD.

The two possible reactions occurring in this dissociation are the following:

The isotopic exchange reaction

$$2\,HD \rightarrow H_2 + D_2 \qquad (1.3.2.5)$$

which is known to occur at higher temperature.

The other reaction is a scavenging of HD by the $H^\bullet$ and $OH^\bullet$ radical from the sonolysis of water.

$$H_2O \rightarrow H^\bullet + OH^\bullet \qquad (1.3.2.6)$$

$$H^\bullet + HD \rightarrow H_2 + D^\bullet \qquad (1.3.2.7)$$

$$OH^\bullet + HD \rightarrow H_2O + D^\bullet \qquad (1.3.2.8)$$

$$OH^\bullet + HD \rightarrow HDO + H^\bullet \qquad (1.3.2.9)$$

The $H^\bullet$ and $D^\bullet$ radicals formed by these reactions also produce H_2 and D_2.

$$2\,H^\bullet \rightarrow H_2 \qquad (1.3.2.10)$$

$$2\,D^\bullet \rightarrow D_2 \qquad (1.3.2.11)$$

1.4. Aims of the Study

As indicated above, the production of nitrogen fertilizer requires overall extreme conditions in the formation of ammonia.

The eventual aim of this research is to see if ultrasonic irradiation of liquids saturated with N_2 and other appropriate gases can result in sufficiently effective nitrogen fixation to have commercial applications. This is why the experiments were extended to ammonia formation in alkanes with N_2/H_2 mixtures. Such sonication systems could be used with a catalyst to increase the rate of ammonia production.

2. Thermodynamics and Kinetics

2.1. Nitrite and Nitrate

Two important nitrogen oxides in producing nitrous and nitric acids are NO and NO_2. In the gas phase, the presence of both oxides and vapour water will result in the formation of nitrous acid [Asquith and Tyler, 1970].

$$NO_{(g)} + NO_{2(g)} + H_2O_{(g)} = 2\,HNO_{2(g)}\,; \quad K(20^{\circ}C) = 1.56\ atm^{-1} \qquad (2.1.1.1)$$

Aqueous solutions of nitrous acid are unstable and decompose reversibly when heated:

$$3\,HNO_{2(aq)} = HNO_{3(aq)} + 2\,NO + H_2O_{(l)} \qquad (2.1.1.2)$$

Based on this reaction, nitrous acid solutions can behave as both oxidizing and reducing agents, e.g., towards I^-, Fe^{+2} and $C_2O_4^-$ [Green and Sykes, 1970]:

Oxidizing agent:

$$HNO_{2(aq)} + H^+_{(aq)} + e_{(aq)} = NO_{(aq)} + H_2O_{(l)}\,; \quad E^o = 1.0\ V \qquad (2.1.1.3)$$

Reducing agent:

$$NO_3^-{}_{(aq)} + 3\,H^+_{(aq)} + 2e_{(aq)} = HNO_{2(aq)} + H_2O_{(l)}\,; E^o = 0.94\ V \qquad (2.1.1.4)$$

Nitrate is one of the components of fertilizer; other common components are urea, ammonium sulphate, potassium ammonium nitrate, superphosphates and ammonium phosphate, potassium chloride, and potassium sulphate [Faust, et al., 1999]. The reaction for formation of nitric acid is:

$$3\,NO_{2(g)} + H_2O_{(l)} = 2\,HNO_{3(aq)} + NO_{(g)}\,; \quad \Delta_rG^{\theta} = -5.0\ kJ\ mol^{-1} \qquad (2.1.1.5)$$

Production of nitric acid is obtained industrially through the Ostwald process [Cotton and Wilkinson, 1972; Shriver and Atkins, 1999]. In this process, the NO_2 is obtained from oxidizing ammonia rather than from the direct reaction of N_2 and O_2. This is because the direct reaction of N_2 and O_2 is unfavourable thermodynamically at ambient temperature:

$$0.5\ N_{2(g)} + O_{2(g)} = NO_{2(g)};\quad \Delta_r G^{\theta} = 51\ kJ\ mol^{-1} \qquad (2.1.1.6)$$

However,

$$4\ NH_{3(g)} + 7\ O_{2(g)} = 4\ NO_{2(g)} + 6\ H_2O_{(l)};\ \Delta_r G^{\theta} = -308.0\ kJ\ mol^{-1} \qquad (2.1.1.7)$$

The by-product NO in equation (2.1.1.5) is then oxidized for a recycling process.

2.2. The Solubility of Gases

The solubility equations of compounds of interest in water are given below:

Nitrogen gas, at a partial pressure of 1.0 atm, temperature range from 273 K to 350K, standard deviation in the mol fraction of gas in solution, x_g = 0.72 % [Battino et al., 1984]:

$$\ln x_g = -181.5870 + 8632.13/(T/K) + 24.7981\ \ln(T/K) \qquad (2.2.1)$$

Oxygen gas, at a partial pressure of 1.0 atm, temperature range from 273 K to 333 K, standard deviation in x_g = 0.17 % [Battino et al., 1981]:

$$\ln x_g = -171.2542 + 8391.24/(T/K) + 23.24323\ \ln(T/K) \qquad (2.2.2)$$

Hydrogen gas, at a partial pressure of 1.0 atm, temperature range from 273 K to 345 K, standard deviation in x_g = 0.52 % at about 300 K [Wilhelm, 1981]:

$$\ln x_g = -125.939 + 5528.45/(T/K) + 16.8893\ \ln(T/K) \qquad (2.2.3)$$

Partial pressure of NH_3 above a saturated solution, temperature range from 240 K to 371 K [Lange's Handbook of Chemistry, 1979]:

$$\ln(P/bar) = 11.2489 - 2584.9/[(T/K) - 9.49] \qquad (2.2.4)$$

The solubility of the compounds of interest in organic solvents of interest are given below [Makranczy et al., 1976; Tremper and Prausnitz, 1976]:

Table. 2.2.1. The solubility of compounds of interest in organic solvents of interest

Organic	T (K)	$x_g(H_2)$	$x_g(N_2)$	$x_g(O_2)$	$x_g(NH_3)$
Heptane	298.2	0.00066	0.00138	0.00194	-
Octane	298.2	0.00064	0.00133	0.00190	-
Hexadecane	298.2	0.00072	0.00126	-	0.0218

Table 2.2.1 indicates that there is not much variation (< 10%) of the solubility of the gases in the various alkanes, at least not on a mol fraction basis. Ammonia is quite soluble in alkanes relative to N_2 and H_2.

The solubility equations for gases of interest in specific organic solvents are given below [Byrne et al., 1974; Battino et al., 1984]:

Nitrogen gas, at a partial pressure of 1.0 atm, temperature range from 280 K to 333K, standard deviation in $ln\ x_g$ = 0.0.0090, in benzene:

$$\ln x_g = -6.0544 - 495.67/(T/K) \qquad (2.2.5)$$

Hydrogen gas, at a partial pressure of 1.0 atm, temperature range from 248 K to 308 K, standard deviation in x_g = 0.00000308, in octane:

$$\ln x_g = -5.6624 - 484.38/(T/K) \qquad (2.2.6)$$

2.3. Thermodynamics

2.3.1. Fundamental Data

Fundamental thermodynamic data are readily available [HCP, 1999] for all the species involved, except the $OH^{\bullet}$ radical. For the dissociation of water, the standard enthalpy

was thus taken as the dissociation energy of H-OH bond (495 kJ mol^{-1} [Herzberg, 1950]); this compares with the suggested activation energy of 440 kJ mol^{-1} for the dissociation of water [Hart and Henglein, 1986]. The absolute entropy for $OH^{\bullet}$ was assumed to be 170 J K^{-1} mol^{-1}, approximately that for HF.

For the standard state, at 298 K, the $\Delta_f G^{\theta}$, $\Delta_f H^{\theta}$ and S^{θ} of the compounds of interest are given below [HCP, 1999; Atkins, 1998]:

Table.2.3.1.1. Fundamental data for compounds of interest

	$\Delta_f H^{\theta}$ (kJ mol^{-1})	S^{θ} (J mol^{-1} K^{-1})	$\Delta_f G^{\theta}$ (kJ mol^{-1})
N_2	0	191.61	0
O_2	0	205.138	0
H_2	0	130.684	0
NO	90.25	210.76	86.55
NO_2	33.18	240.06	51.31
NH_3	-46.11	192.45	-16.45
H_2O	-241.82	188.83	-228.57
H	218.00	114.72	203.25
N	472.68	153.30	455.56
O	249.18	161.06	231.73
OH	495.	170.	444.

The temperature dependence of $\Delta G^{0}_{(T)}$ for ammonia formation is given in cal mol^{-1} by Lewis and Randall, 1923, as:

$$N_{2(g)} + 3\ H_{2(g)} = 2\ NH_{3(g)}$$

$$\Delta G^{0}_{(T)} = -9500 + 4.96\ T \ln T + 0.000575\ T^2 - 0.00000085\ T^3 - 9.16\ T \qquad (2.3.1.1)$$

2.3.2. Calculations of Equilibrium Constants

Any thermodynamic analysis for temperatures as high as 5000 K is necessarily very approximate, as data are not available to make the corrections for temperature dependence of the standard enthalpy and entropy differences. The situation in an imploding cavity is also far different from the ideal gas conditions assumed in the elementary thermodynamics used here.

The effect of temperature on the equilibrium constant for formation of NO and NO_2 is given below [Yen, 1999]:

$$N_2 + O_2 = 2\ NO \qquad (2.3.2.1)$$

$$K = p^2(NO) / [p(N_2)\ p(O_2)] = Y^2(NO) / [Y(N_2)\ Y(O_2)] \qquad (2.3.2.2)$$

$$K = 10^{-30}\ (\text{at } 300K) = 7.5 \times 10^{-9}\ (\text{at } 1000K) = 4.0 \times 10^{-4}\ (\text{at } 2000K) \qquad (2.3.2.3)$$

$$NO + 0.5\ O_2 = NO_2 \qquad (2.3.2.4)$$

$$K = p(NO_2) / [p(NO)\ p(O_2)^{0.5}] = P_t^{\ 0.5}(YNO_2) / [Y(NO)\ Y(O_2)^{0.5}] \qquad (2.3.2.5)$$

$$K = 10^{6}\ (\text{at } 300K) = 1.2 \times 10^{2}\ (\text{at } 1000K) = 3.5 \times 10^{-3}\ (\text{at } 2000K) \qquad (2.3.2.6)$$

Here p = partial pressure in atm, P_t = total pressure in atm, Y = mol fraction.

These data show that the formation of NO is favoured at high temperature. The formation of NO_2 from NO, on the other hand, is less favoured at high temperature.

It should be noted that the K values calculated in 2.3.2.3 and 2.3.2.6 refer to fugacities (activities). Moreover, they are calculated assuming ΔH^{θ} and ΔS^{θ} to be temperature independent. Because of the high pressures present in an imploding cavity, partial pressures can be substantially different from fugacities. There would also be a substantial change in the ΔH^{θ} and ΔS^{θ} of reactions over the range of thousands of degrees Kelvin. Thus partial pressures calculated from these K values should be considered as order of magnitude values only.

The complete thermodynamic calculations as a function of temperature for all species of interest are summarized in the following sections:

2.3.2.1. Dissociation of H_2 gas

$$H_2 = H^{\bullet} + H^{\bullet}$$

Table 2.3.2.1. Thermodynamic estimates of concentration of $H^{\bullet}$ radicals. The numbers shown are estimated equilibrium partial pressure (atm) assuming the pressure of H_2 be 100 atm. Data are from section 2.3.1.

T (K)	$\Delta_f G^{\theta}$ (kJ mol^{-1})	K	p($H^{\bullet}$) atm
298	406.57	5.45×10^{-72}	2.3×10^{-35}
673	369.53	2.09×10^{-29}	4.5×10^{-14}
2000	238.49	5.92×10^{-7}	$8. \times 10^{-3}$
5000	-57.77	4.01	20.

Thus at 5000 K, the concentration of $H^{\bullet}$ should be considerable as the degree of dissociation of H_2 is in the order of 10%.

2.3.2.2. Dissociation of N_2 gas

$$N_2 = N^\bullet + N^\bullet$$

Table 2.3.2.2. Thermodynamic estimates of concentration of $N^\bullet$ radicals. The numbers shown are estimated equilibrium partial pressure (atm) assuming the pressures of N_2 be 100 atm. Data are from section 2.3.1.

T (K)	$\Delta_r G^\theta$ (kJ mol^{-1})	K	p($N^\bullet$) atm
298	910.50	0	0
673	866.62	5.51×10^{-68}	2.3×10^{-33}
2000	711.37	2.64×10^{-19}	$5. \times 10^{-9}$
5000	360.39	1.72×10^{-4}	0.1

The ratio of $H^\bullet$ to $N^\bullet$ atoms in an imploding cavity is thus likely to be the order of 200 (i.e. 20/0.1) at 5000 K.

2.3.2.3. Ammonia formation

$$N_2 + 3\,H_2 = 2\,NH_3$$

Table 2.3.2.3.1. Thermodynamic estimates of concentration of NH_3. The numbers shown are estimated equilibrium partial pressure (atm) assuming the pressures of N_2 and H_2 to both be 100 atm. Data are from section 2.3.1.

T (K)	$\Delta_r G^\theta$ (kJ mol^{-1})	K	p(NH_3) atm
298	-15.82	589.92	2.4×10^5
673	25.41	0.010	1000
2000	180.25	1.96×10^{-5}	44.
5000	267.99	1.58×10^{-3}	400.

This reaction is the only one of those listed in the tables in section 2.3.2 for which the equilibrium favours products at lower temperature. It is the only exothermic reaction.

The variation of K at high temperature may not be correct as K has a minimum with T. This is most likely due to the equation (2.3.1.1) being invalid at such high temperature; a temperature range of validity for this equation was not given. Table 2.3.2.3.2 is thus also presented. It assumes $\Delta_r G^\theta = \Delta_r H^\theta(298\ K) - T\Delta_r S^\theta(298\ K)$

Table 2.3.2.3.2. Thermodynamic estimates of concentration of NH_3. The numbers shown are estimated equilibrium partial pressure (atm) assuming the pressures of N_2 and H_2 to both be 100 atm. Data are from section 2.3.1.

T (K)	$\Delta_r G^\theta$ (kJ mol^{-1})	K	p(NH_3) atm
298	-33.00	6.03×10^5	7.8×10^6
673	41.55	0.020	1414
2000	305.30	1.06×10^{-8}	1.0
5000	901.58	3.80×10^{-10}	0.2

2.3.2.4. NO Formation

$$N_2 + O_2 = 2\,NO$$

Table 2.3.2.4. Thermodynamic estimates of concentration of NO. The numbers shown are estimated equilibrium partial pressure (atm) assuming the pressures of N_2 and O_2 to both be 100 atm. Data are from section 2.3.1.

T (K)	$\Delta_r G^\theta$ (kJ mol^{-1})	K	p(NO) atm
298	173.12	4.53×10^{-31}	6.7×10^{-14}
673	163.83	1.92×10^{-13}	4.4×10^{-5}
2000	130.96	3.78×10^{-4}	2.
5000	56.65	0.26	50.

The value at 2000 K agrees with that given by Yen [1999].

2.3.2.5. NO_2 Formation

$$N_2 + 2\,O_2 = 2\,NO_2$$

Table 2.3.2.5. Thermodynamic estimates of concentration of NO_2. The numbers shown are estimated equilibrium partial pressure (atm) assuming the pressures of N_2 and O_2 to both be 100 atm. Data are from section 2.3.1.

T (K)	$\Delta_r G^\theta$ (kJ mol^{-1})	K	p(NO_2) atm
298	102.65	1.02×10^{-18}	1.0×10^{-6}
673	148.31	3.07×10^{-12}	1.7×10^{-3}
2000	309.90	8.03×10^{-9}	0.1
5000	675.21	8.85×10^{-8}	0.3

The formation of NO is thus favoured over the formation of NO_2 by a factor of 50/0.3.

2.3.2.6. $OH^{\bullet}$ Formation

$$H_2O = H^{\bullet} + OH^{\bullet}$$

Table 2.3.2.6. Thermodynamic estimates of concentration of $OH^{\bullet}$. The numbers shown are estimated equilibrium partial pressure (atm) assuming the pressures of H_2O to be 100 atm. Data are from section 2.3.1.

T (K)	$\Delta_r G^{\theta}$ (kJ mol^{-1})	K	$p(OH^{\bullet})$ atm
298	926.24	0	0
673	890.19	8.0×10^{-70}	2.8×10^{-34}
2000	763.04	$1. \times 10^{-20}$	$1. \times 10^{-9}$
5000	475.37	$1. \times 10^{-5}$	0.03

The dissociation of H_2O to $H^{\bullet}$ and $OH^{\bullet}$ in implosion of cavities is well-documented [Reisz et al., 1985; Mason et al., 1994]. The dissociation of N_2 to $2N^{\bullet}$ is thus also likely as simple thermodynamics show this to be more favourable at 5000 K (see table 2.3.2.2). The degree of dissociation of water at 5000 K is in the order of 0.03%, while that of N_2 is in the order of 0.05%.

2.4. Kinetics of NO_x Formation

Reaction between O_2 and N_2 produces NO_x. The nitrogen oxides NO_x consist of N_2O, NO, NO_2, N_2O_3, N_2O_4, and N_2O_5. Of those six oxides, the most important two

are NO and NO_2, especially in producing nitrous and nitric acids.

In combustion in an engine, NO production is believed to occur by the "Zeldovich" mechanism [Yen, 1999]:

$$N_2 + O \rightarrow NO + N \quad (2.4.1)$$

$$N + O_2 \rightarrow NO + O \quad (2.4.2)$$

$$N + OH \rightarrow NO + H \quad (2.4.3)$$

The concentration of NO in engine combustion can be calculated with the equation below:

$$C_{NO}\,(ppm) = 5.2 \times 10^{17} [\exp(-72300/T)]\, Y(N_2) Y^{0.5}(O_2)\, t \quad (2.4.4)$$

Here, T = absolute temperature in K, Y = mole fraction, and t = time in second.

In spark-ignition engines, the formation of NO_2 is negligible compared to NO. In a diesel engine, however, it is a significant amount, in the range of 10 to 30 percent of the total exhaust oxides of nitrogen emission [Heywood, 1988]. The proposed mechanism of formation of NO_2 is given below:

$$NO + HO_2 \rightarrow NO_2 + OH \quad (2.4.5)$$

$$NO_2 + O \rightarrow NO + O_2 \quad (2.4.6)$$

When NO_2 is formed, mixing with cooler fluid immediately quenches it. As result the forward reaction in (2.2.6) is very slow. This explains why the ratio of NO_2 / NO yield is high.

Experimental Methods

3.1. Materials

Materials used in this experiment were grouped as solids, liquids and gases. The materials in each of these groups are given below:

3.1.1. Solids

A number of solids were required to make solutions for calibrations and to make ionic strength solutions:

Ammonium chloride (NH_4Cl, F.W. 53.49), Aldrich Chemical Co, Inc, USA, 99.99% purity, Catalogue number 32,637-2.

Ammonium sulfate ($(NH_4)_2SO_4$, F.W. 132.14), Fisher Scientific Co, USA, 21.09% total nitrogen content, CAS 7783-20-2, Lot number 976268.

Iodine (Chips), Aldrich Chemical Co, Inc, USA, 99+% purity, Catalogue number 37-655-8.

Potassium chloride (KCl, F.W. 74.55), J.T. Baker Chemical Co, Phillipburg, 99.8% purity, Catalogue number 1-3040.

Potassium iodide (KI, F.W. 166.01), Aldrich Chemical Co, Inc, USA, 99% purity, Catalogue number 20,796.9.

Potassium nitrate (KNO_3, F.W. 101.11), Fisher Scientific Co, USA, 13.83% total nitrogen content, CAS 7757-79-1, Lot number 975412A.

Sodium chloride (NaCl, F.W. 58.44), BDH Chemicals, Toronto, 99.9% purity, Catalog number 54971/6519.

Sodium nitrite ($NaNO_2$, F.W. 69.00), Fisher Scientific Co, USA, 99.8% purity CAS 7632-00-0, Lot number 980393.

Sodium sulfite (Na_2SO_3, F.W. 103.05), Aldrich Chemical Co, Inc, USA, 98+% purity, Catalogue number 23,932-1.

3.1.2. Liquids

Deionized water, available at Carleton University's laboratory. This was used for sonochemical experiments.

Deionized water from Millipore apparatus S.A 67120 Malshein, France, catalogue number D 5311595, serial number FOJM 678586. This was used for making up standard solutions.

Nessler's reagent, Aldrich Chemical Co, Inc, USA, 1.097 densities, Catalogue number 34,514-8. This was used for spectrophotometric analysis of ammonia (Appendix D.1).

There were four buffer solutions used in this experiment. They were used for calibration of the pH electrode. The characteristics of each of these solutions are given below:

pH (1.98 – 2.02) at 25°C, Anachemia Canada Inc., Lot number R-1160, UN-1760.

pH (3.00 ± 0.02) at 25°C, Fisher Scientific Co, USA, Lot number SO-B-97.

pH (6.99 – 7.01) at 25°C, Anachemia Canada Inc, Lot number R-1230.

pH (10.00 ± 0.02) at 25°C, Anachemia Canada Inc.

Hydrogen peroxide solution (H_2O_2, F.W. 34.02), Aldrich Chemical Co Inc, USA, 30wt% purity, Catalog number 21,676-3. This was used to oxidize the nitrite to nitrate (Appendix B.3).

A solution of ($NH_4)_2SO_4$, 2.0 M as ionic strength adjustor in measuring nitrate ion concentrations (Appendix B.1).

A solution of KI_3, 0.10 M made by dissolving solid iodine into KI solution. This was for obtaining a calibration graph for determination of ultrasonic power (Appendix E.1).

Potassium iodide solution, 0.20 M.

Potassium nitrate solution, 0.10 M.

Sodium nitrite solution, 0.10 M.

These calibration solutions were prepared from solid materials that are listed in 3.1.1 with deionized water from the Millipore apparatus.

Octane (F.W. 114.23), Aldrich Chemical Co., Inc., USA, 98% purity, Catalogue number 41, 223-6. It was used in some experiments for ammonia formation (see section 4.3). It was chosen as alkanes are relatively inert to sonolysis and as it has a suitable vapour pressure.

3.1.3. Gases

The following gases were used to sparge through the sonochemical reaction:

Compressed air was available at Carleton University's laboratory.

Hydrogen gas, Canadian Oxygen Limited, Missisauga, Ontario with labeling CANOX.

Nitrogen gas, BOC Canada Limited, Missisauga, Ontario.

Oxygen gas, grade 4.4, BOC Canada Limited, Missisauga, Ontario.

3.2. Equipment

The equipment to carry out the experiments is described below:

3.2.1. Electrochemical Measurements

The primary method for analysis of sonochemical products was electrochemical. Three type electrodes were used in this experiment:

Single junction reference electrode, Model 901-01, Orion Research Inc.

Single junction pH electrode, Accumet model, Fisher Scientific Co, USA, Catalog number 13-620-108.

Nitrate electrode, Orion Research Inc., Boston, USA, Lot number AW1, for a 10^{-4} M solution of NO_3^-, there is a 10% error due to interference of NO_2^- at an NO_2^- concentration of $7x10^{-5}$ M.

The potentiometer used for all electrochemical measurements was a pH meter, model 950, Fisher Scientific Co, U.S.A.

3.2.2. Other Equipment

Matheson Gas products Rotameter or flow meter, Model 7630T-602

Thermostat, Brinkmann Instruments, Lauda K-2/R A sparging mechanism for air or gas mixtures of N_2 and O_2, as shown in fig. 3.2.2.1 (see section 3.3.3 for the procedure used).

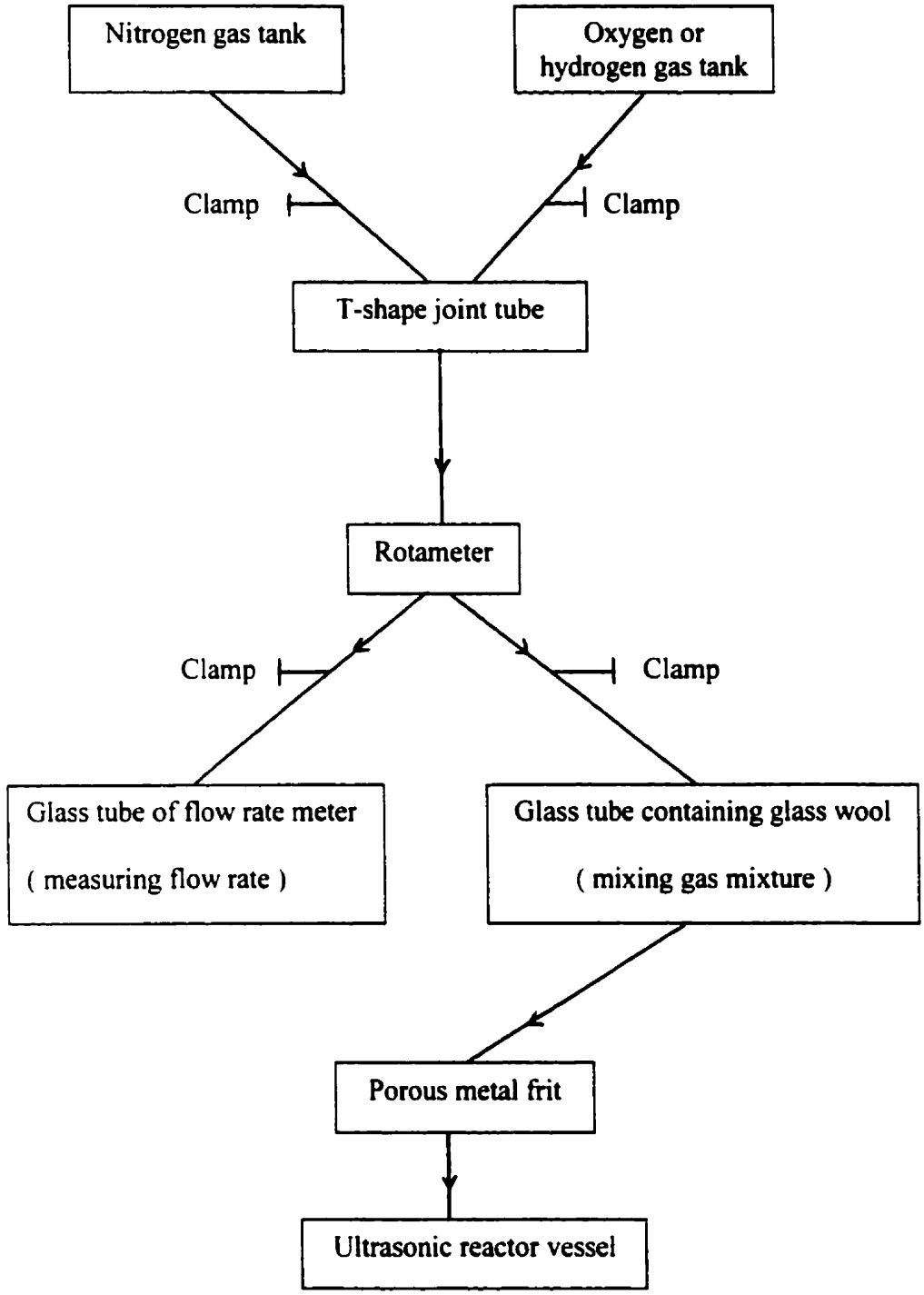

Figure 3.2.2.1. Schematic of gas introduction. Rotameter calibration graphs are in appendix A.1.

3.2.3. Spectrophotometers

Spectrophotometers were required to analyze for ammonia using Nessler's reagent (Appendix D.1), and for power calibration (Appendix E.1). These were a Spectronic 21 and a Perkin-Elmer lambda 4B UV-Visible spectrophotometers.

3.2.4. 900 kHz Sonochemical Reactor

This equipment was developed by M. Entezari in his Ph.D. research and was available for use at the beginning of this project. It is described by Entezari and Kruus, [1994] (see figure 3.2.4.1), and in more detail in Mohammad H. Entezari's Ph.D. thesis (The Effect of Frequency on Sonochemical Reactions) at Carleton University, 1994. The liquid sits on the top of a fragile piezoceramic transducer in this reactor.

3.2.5. 850 kHz Sonochemical Reactor

An apparatus was constructed during this research project. It produces 850 kHz ultrasound through a flat transducer covered by titanium situated at the top of a reaction vessel holding the solution. The details of the sonication cell are shown in Figure 3.2.5.1.

The transducer was from Meinhardt Ultrasonics, Leipzig, Germany (Figure 3.2.5.2). It was less fragile than the 900 kHz transducer as it was in a titanium body. It is thus possible to operate in the highest power mode from an amplifier during sonication. It is also more portable, so that it is easy to do an experiment directly outside, such as for ground water. The frequency generator and amplifier for this apparatus were the same as those used by Entezari and Kruus (Figure 3.2.5.3).

In this new apparatus, the ultrasound can enter any system directly as nearly any liquid can contact the titanium. Before irradiation, it is necessary to make sure that the transducer is immersed completely in the system to avoid loss of power.

During sonication, heat is dissipated in the solution. The sonication cell was thus equipped with a circulating water bath for controlling temperature.

Experiments using solid catalysts are also possible with this equipment. The catalyst is paced on a platinum screen mounted in the middle of circular copper platform in the reaction vessel.

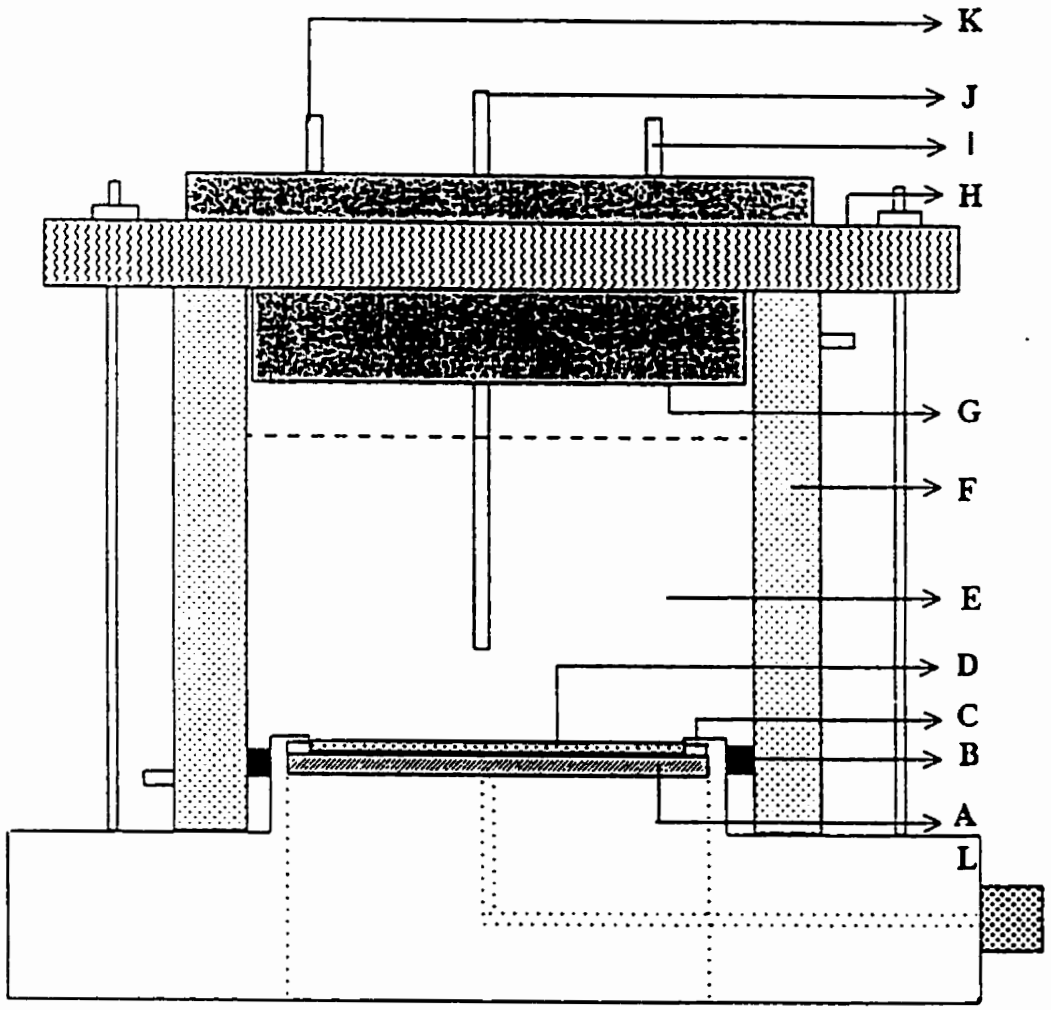

Figure 3.2.4.1: Sonochemical reactor which designed and constructed for 900 kHz apparatus (after Entezari and Kruus, 1994)

A: transducer (EBL#1 (PZT-4) 2.125 in diameter from Staveley Sensors Inc. Connecticut), B: O ring (Buna-N), C: silver conducting epoxy cement (chomerics). D: propective resin (RTV 11 white), E: reaction solution (typically 150 mL), F: circulating thermostating bath, G: lid (plastic), H: support frame (plastic), I: entry for thermocouple, J: inlet for gases (stainless steel tube with a perforated end), K: outlet for gases, L: stainless steel base.

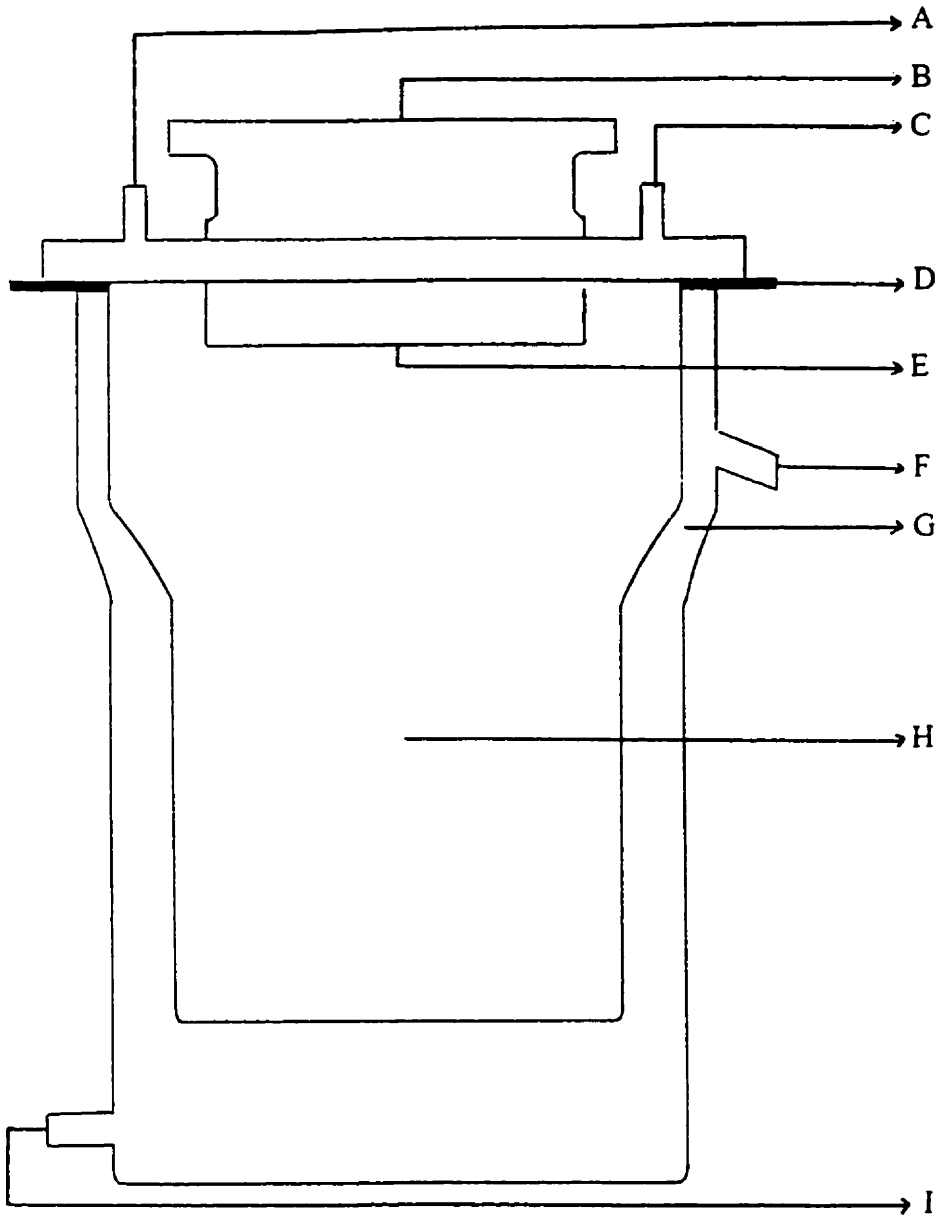

Figure 3.2.5.1: Sonochemical reactor which designed and constructed for 850 kHz apparatus (after Entezari and Kruus, 1994)

A: Outlet gases, B: stainless steel support of transducer, C: inlet for gases, D: aluminum support, E: transducer, F: outlet for cooler, G: circulating thermostating bath, H: reaction solution (typically 380 mL), I: inlet for cooler.

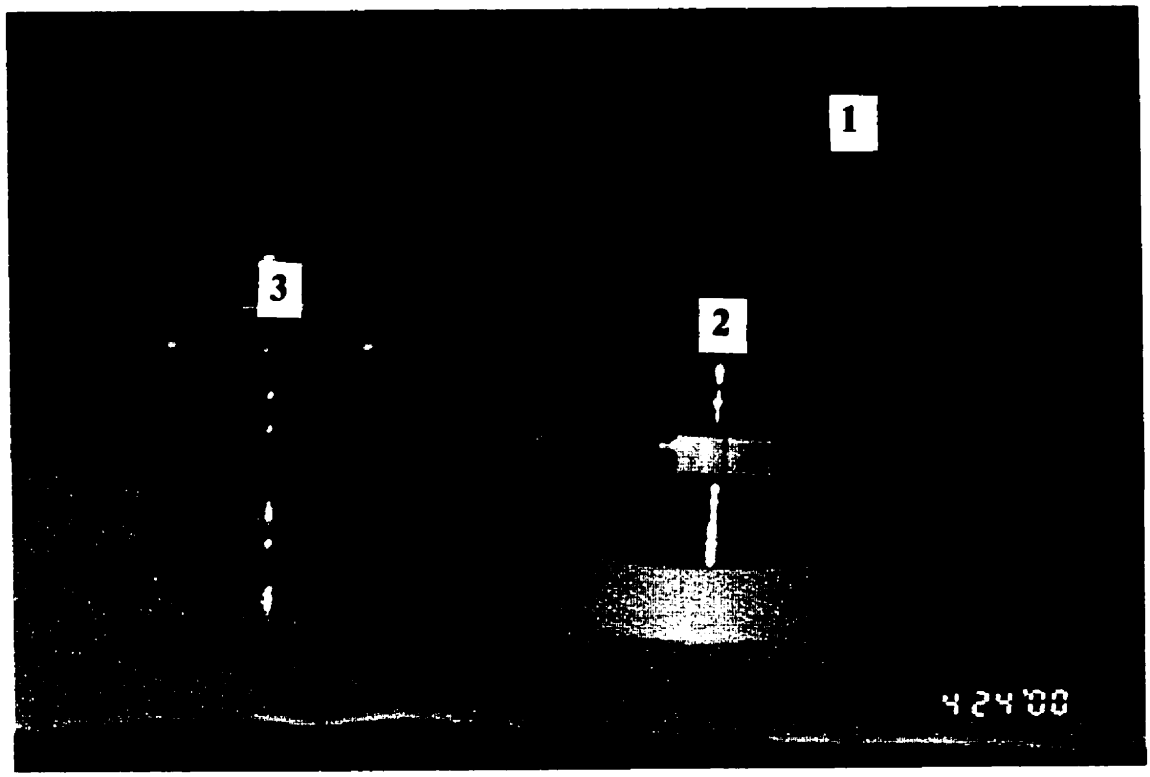

Figure 3.2.5.2: 850 kHz of transducer apparatus from Meinhardt Ultrasonics, Leipzig, Germany and reaction chamber.

Porous metal frit to intoduce gas (1), transducer suface (2), and reaction chamber (3).

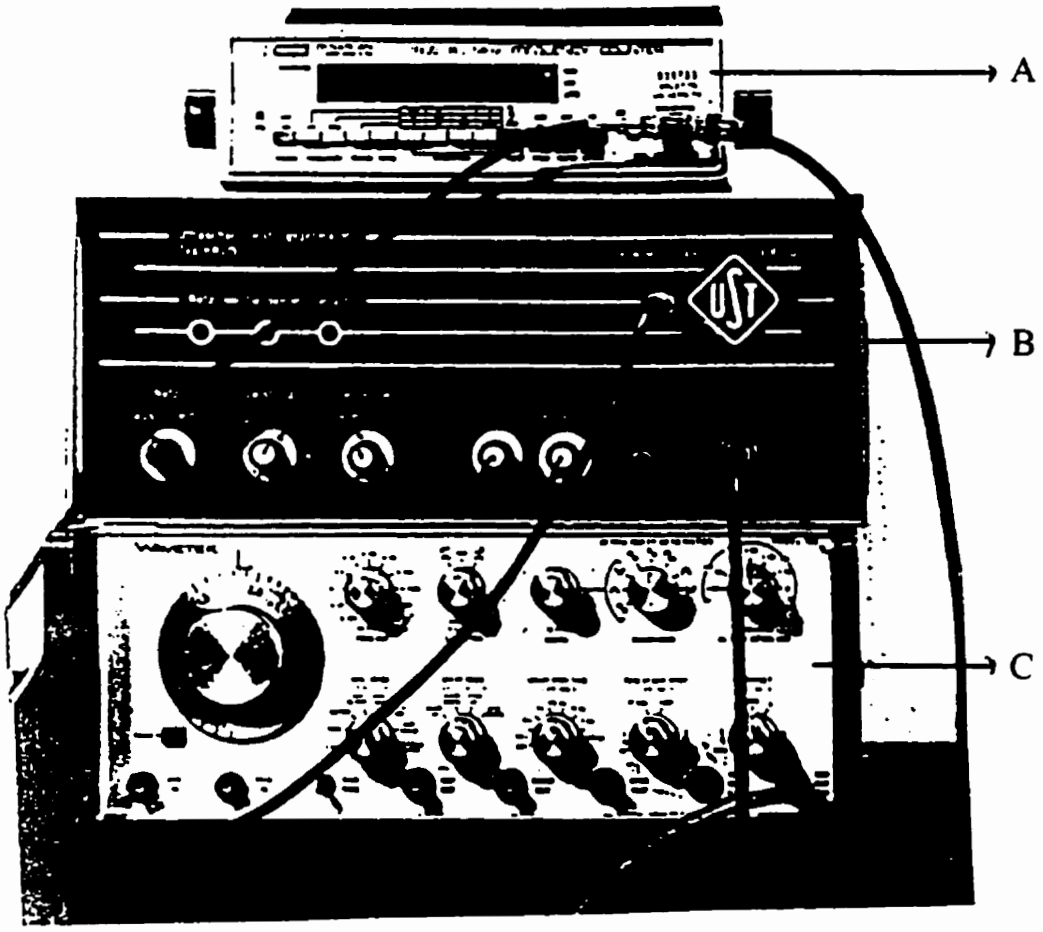

Figure 3.2.5.3: 900 kHz and 850 kHz apparatus (power amplifier from an apparatus supplied by Meinhardt Ultrasonics).

A: frequency counter, B: power amplifier, C: frequency generator.

3.3. Procedure

Immediately prior to use, all glass equipment was cleaned sequentially as follows: a detergent wash, tap water rinse, deionized water rinse (6 times) and drying.

There were two methods for irradiating deionized water by ultrasound, with sparging air or gas into the ultrasonic chamber, and without any air or gas. Unless otherwise stated, the temperature of the chamber was kept constant at 5°C with an outside thermostat. This was the lowest possible operating temperature, and the rate of reaction increased with decreasing temperature (see section 4.1.5).

3.3.1. Irradiation of Deionized Water by 900 kHz Ultrasound without Sparging Air or Gas

Before irradiation, a 50, 100 or 200 mL sample of deionized water was measured for its pH, then poured into the ultrasonic chamber, which was loosely covered by aluminum foil. When the temperature of the deionized water reached 5 ± 2°C, ultrasonic irradiation was started and then stopped after specific times (5, 10, 20, 40, 60, 120 and 180 minutes). After that, the water was collected in a glass beaker and the pH was measured. Experiments were done in triplicate, unless otherwise stated.

3.3.2. Irradiation of Deionized Water by 900 kHz Ultrasound with Sparging Air

After measuring the pH of a sample of 100 mL water and pouring it into an ultrasonic chamber, air was sparged by a porous metal frit in the chamber which was tightly closed with a teflon plug. The flow rate of air into the chamber was determined by a flow rate meter in units of mL per second. Irradiation was conducted when the temperature

inside the chamber attained 5 ± 2°C and stopped in 20 minutes. The water was collected in a beaker and its pH measured. The flow rate of air was varied; the highest concentration of H^+ (lowest pH) was obtained for a flow rate of air of 2.9 mL s^{-1} (see 4.1.1.3). This was used as the total flow rate for mixtures of nitrogen and oxygen or hydrogen gases for sparging the water in the ultrasonic chamber.

3.3.3. Irradiation of Deionized Water while Sparging with a Gas Mixture for 900 kHz

With the same procedure as in (3.3.2), a mixture of nitrogen and oxygen or hydrogen gases was sparged into a 100 mL sample of deionized water in the ultrasonic chamber.

The steps for determination of flow rate for each gas using equipment described in figure 3.2.2.1 are the following: All gas routes were opened except gas tanks and the connection between rotameter and glass tube containing glass wool. A flow rate of nitrogen gas, for example, the nitrogen gas tank was measured by opening gently, with the other gas tank still closed, for a certain flow rate that can be monitored by the height of metal bits inside of rotameter or the flow rate of soap bubbles inside the bubble flow rate meter. A timer was used to record the flow rate of a soap bubble that was driven by the nitrogen gas. The fixed rate of nitrogen gas needed was determined by adjusting the gas clamp of regulator. With the same procedure as for nitrogen gas, the flow rate of the other gas (oxygen or hydrogen) was determined. After a fixed gas composition was determined, this gas mixture was bubbled into the solution in the reaction vessel by opening the connection between the rotameter and the glass tube containing glass wool, and closing the connection from rotameter to the bubble flow rate meter.

The flow rate of each gas of the mixture was varied from one run to another, but

the total flow rate of the mixture was the same, 2.9 mL s^{-1}. Irradiation was carried out after allowing the gas mixture 15 minutes of sparging to replace the air in the water and the space above the deionized water in the ultrasonic chamber.

The pH, the nitrate and ammonium ion concentration of the irradiated water were measured with a pH electrode, a nitrate ion specific electrode, and Nessler's reagent, respectively (see Appendices B, C and D). To determine nitrite ion concentration, 10 mL of hydrogen peroxide solution was added to the 100 mL sample. After 15 minutes of vigorous mixing to oxidize nitrite to nitrate, the water was boiled on a hot plate for 20 minutes to get rid of the residual hydrogen peroxide. The nitrate ion concentration was then determined again, when the temperature of the solution reached room temperature (see Appendix B.3).

3.3.4. Irradiation of Deionized Water and Octane while Sparging with a N_2/H_2 Gas Mixture for 850 kHz Ultrasound

With the same compositions of N_2/H_2 gas mixtures as in procedure (3.3.3), a mixture of nitrogen and hydrogen gases was sparged into a 382 mL sample of deionized water in the ultrasonic chamber (see Figure 2.7.1). Irradiation was carried out after allowing the gas mixture 50 minutes of sparging to replace the air in the water and the space above the deionized water in the ultrasonic chamber. The pH and ammonium ion concentration of the irradiated water was measured with a pH meter (see Appendix C). Spectrophotometric measurements at 396 nm were done after adding Nessler's reagent into ammonia samples (see Appendix D). The reaction of Nessler's reagent with ammonia is the following:

$$2\,K_2HgI_4 + NH_3 + 3\,KOH \rightarrow I\text{-}Hg\text{-}O\text{-}Hg\text{-}NH_2 + 7\,KI + 2\,H_2O$$

Colourless Yellow

For an organic liquid such as octane, a mixture of nitrogen and hydrogen gases with a composition 0.6 mol fraction N_2 was sparged into a 382 mL sample of octane in the ultrasonic chamber. Irradiation was carried out after allowing the gas mixture 50 minutes of sparging to replace the air in the octane and the space above the octane in the ultrasonic chamber. The exiting gas was trapped in 100 mL of hydrochloric acid (1.0×10^{-5} M). The ammonia in the irradiated octane was extracted three times with 20, 15 and 15 mL of hydrochloric acid (1.0×10^{-5} M). The spectrophotometric measurement was done after adding Nessler's reagent into extracted and trapped ammonia samples at 396 nm wave length. It was necessary to wait up to 4 days for the colour of the solution with Nessler's reagent to develop fully. This is probably because the concentrations were very low (10^{-7} to 10^{-4} M), so that the reactions between the reagent and the ammonia were very slow.

A catalyst usually used in Haber-Bosch process was also used in octane. The catalyst was put in a metal platform, where it was situated about 1 cm under the ultrasonic transducer.

Experimental results and discussion

4.1. Mixtures of N_2 and O_2 in water

4.1.1. Reproducibility

4.1.1.1. Hydrogen Ions Produced with and without Bubbling Air in Water

Figure 4.1.1.1 shows the amount of hydrogen ions with and without bubbling air into deionized water as a function of time. Two independent determinations are shown, together with the mean. Studies were done with 27 W of 900 kHz ultrasound at 5°C.

The graph shows that it is not necessary to bubble air into water for long sonication time to increase the yield. The irradiation with 900 kHz does not cause degassing. However, degassing does occur at a lower frequency such as 20 kHz as the cavitation bubbles are larger (equation 1.1.1), and float to the top.

4.1.1.2. The Effect of Different Volumes of Water

Figure 4.1.1.2 shows the amount of hydrogen ions with different volumes of water as a function of time. Three independent determinations are shown, together with the mean. Studies were done with 27 W of 900 kHz ultrasound at 5°C.

The graph shows that the hydrogen ions produced decreased with increasing volume of water. This is probably because the larger volume damps the transducer that was mounted in the bottom of reaction vessel (section 3.2.4). Such an effect would not be present with the 850 kHz apparatus, as there the transducer is at the top (section 3.2.5).

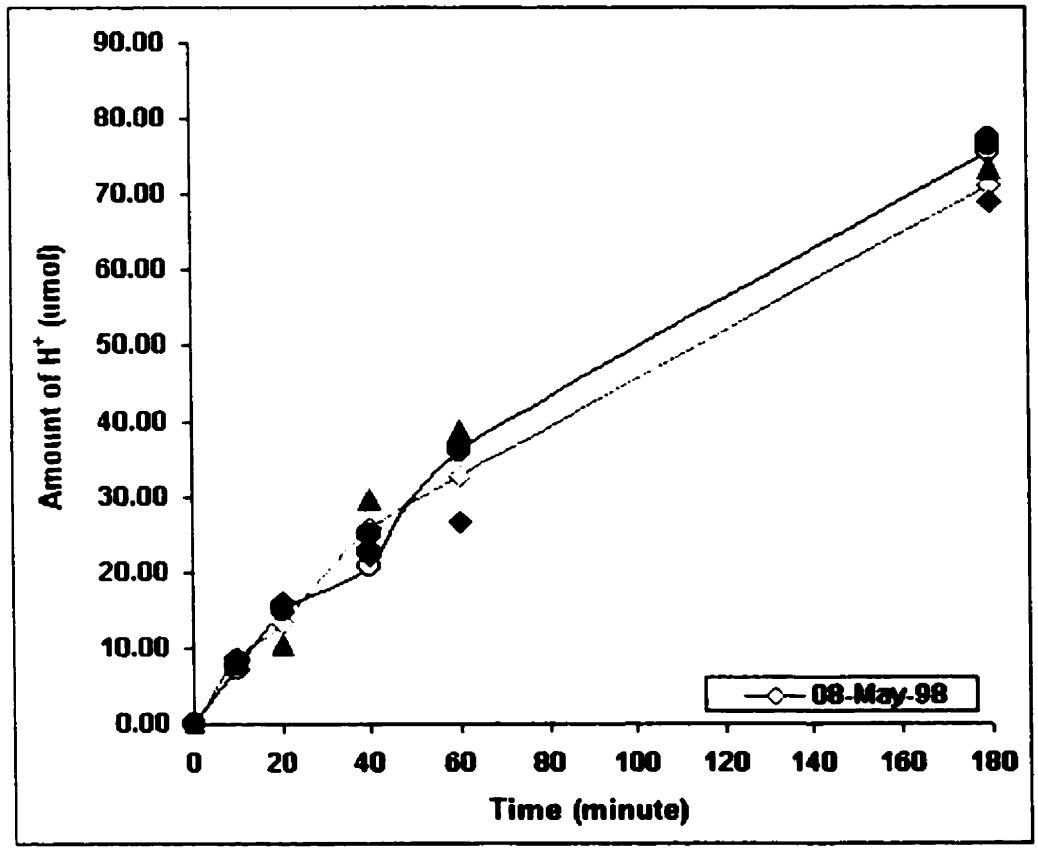

Figure 4.1.1.1. The variation of the amount of hydrogen ions with and without bubbling air into deionized water as a function of time at 5°C. Hydrogen ions with bubbling air (• individual data, O mean), hydrogen ions without bubbling air (♦,▲ individual data, ◊ mean), and power 27 W, 900 kHz irradiation.

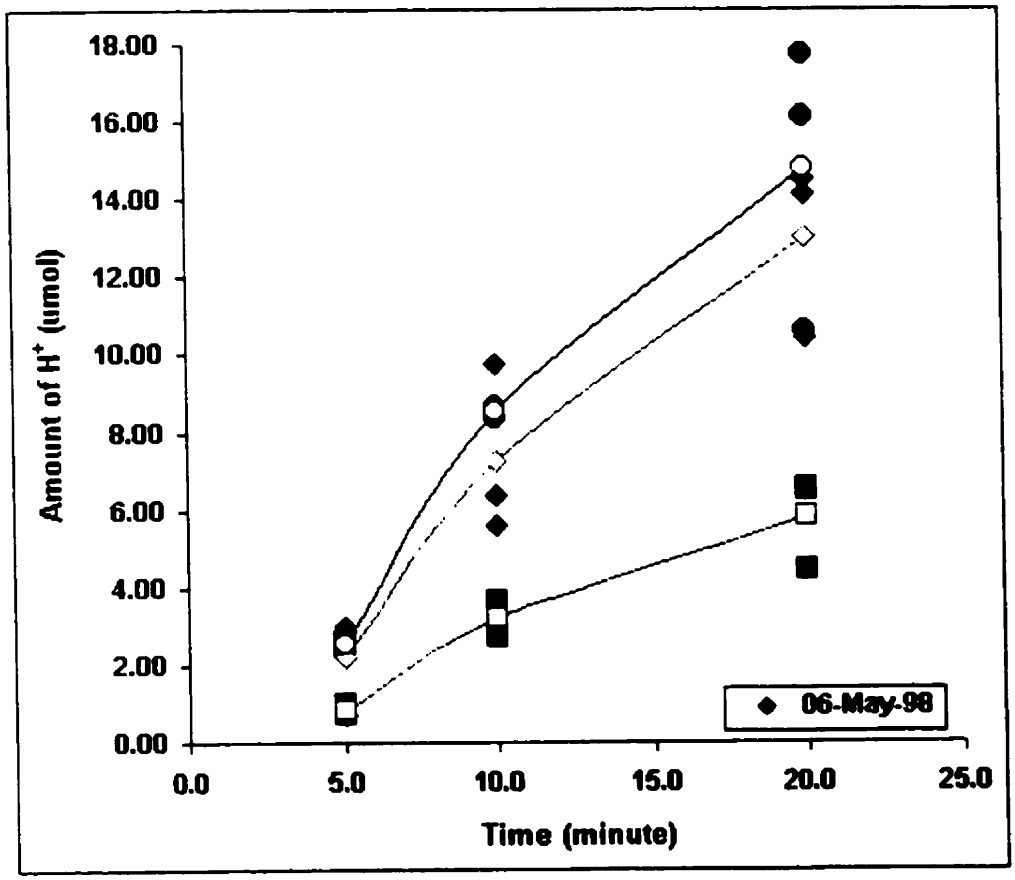

Figure 4.1.1.2. The variation of the amount of hydrogen ions for different volumes of deionized water with time at 5°C. Hydrogen ions for 100 mL (• individual data, O mean), hydrogen ions for 50 mL (●individual data, ◊ mean), hydrogen ions for 200 mL (■ individual data, □ mean). 900 kHz of ultrasound (27 W).

4.1.1.3.The effect of Different Flow Rate of Air

Figure 4.1.1.3 shows the variation of the amount of hydrogen ions with the flow rate of air. Three independent determinations are shown, together with the mean. Studies were done for 20 min with 27 W of 900 kHz ultrasound at 5°C.

There is only a weak dependence of the rate of reaction with flow rate of gases, and as shown in Fig. 4.1.1.1, there is a little difference with zero flow. Nevertheless, the maximum reaction rate was obtained for a flow rate of 2.9 mL s^{-1}. This flow rate was thus used as a total flow rate for a gas mixture of nitrogen/oxygen and nitrogen/hydrogen. It was necessary to have a gas flow in order to control the composition of the dissolved gases and gas bubbles.

4.1.1.4. Hydrogen Ion Measurements and Nitrate

Figure 4.1.1.4 shows the rate of formation of hydrogen and nitrate ions as measured by a pH meter and a nitrate ion specific electrode as function of nitrogen/oxygen gas mixtures. Three independent determinations are shown, together with the mean. Studies were done using 20 min runs with 27 W of 900 kHz ultrasound at 5°C.

The rate of reaction as measured by pH agrees well with that obtained by total nitrate and nitrite. The advantage with using the nitrate ion specific electrode is that it is possible to get the nitrite/nitrate ratio, as well as the total NO_x^-. These data also indicate that the procedure for oxidizing nitrite to nitrate is satisfactory. Judging from the data in Figures 4.1.1.1 to 4.1.1.4, the reproducibility of the N_2/O_2 data is approximately ± 10%.

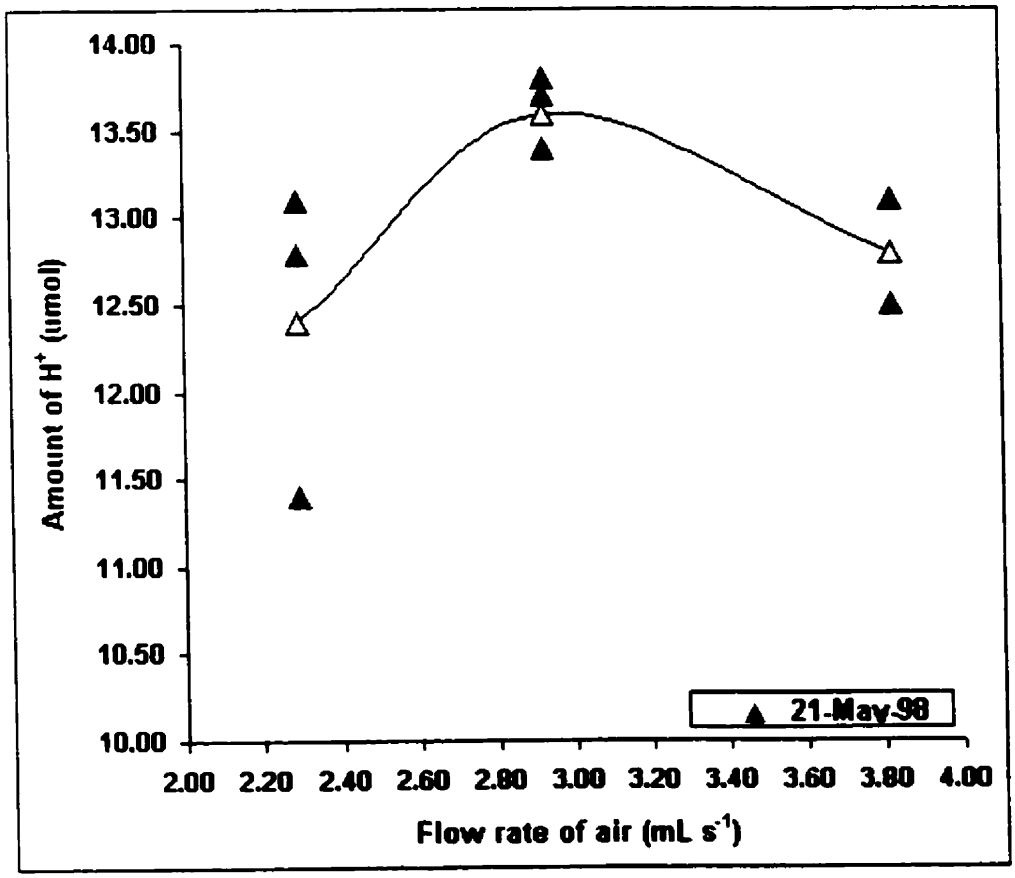

Figure 4.1.1.3. The variation of the amount of hydrogen ions with flow rate of air at 5°C. (▲ individual data, Δ mean), 900 kHz of ultrasound (27 W).

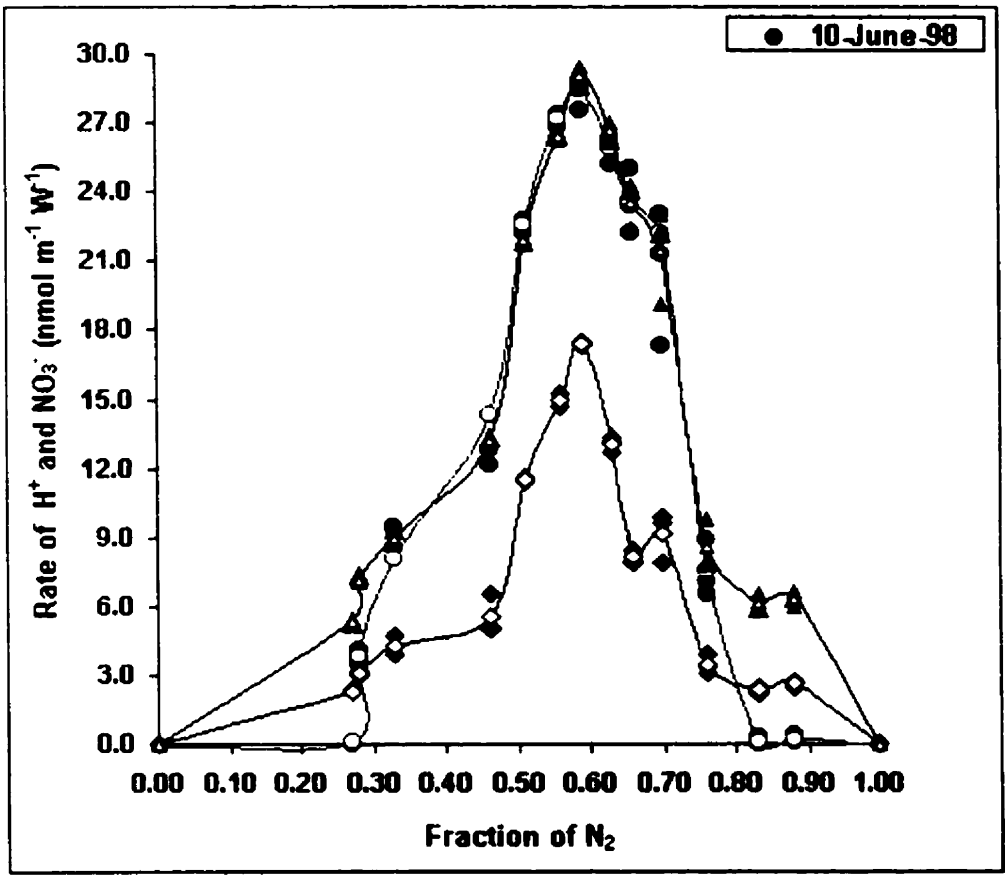

Figure 4.1.1.4. Reproducibility of the rate of formation of nitrate ions and hydrogen ions as a function of composition of N_2 and O_2 gas mixtures (power 27 W, 900 kHz irradiation at 5°C). Total nitrate plus nitrite ions after oxidized by hydrogen peroxide (▲ individual data, Δ mean), hydrogen ions (• individual data, O mean), and initial nitrate ion (♦ indivual data, ◊ mean).

4.1.2. Rate of Nitrite and Nitrate Formation

The highest rate obtained of total nitrate plus nitrite (NO_x^-) in this study can be seen in Fig.4.1.1.4 to be 30 x 10^{-9} mol min^{-1} W^{-1}. The agreement with other investigators is reasonable: 28, 46 and 33 x 10^{-9} mol min^{-1} W^{-1} by Mead et al. [1976], Tiehm [1999], and Petrier et al. [1999], respectively. A higher rate would be expected in this investigation, as an optimal nitrogen/oxygen gas mixture was used, and a lower temperature. However, the frequency used here is not as favourable [Tiehm, 1999].

Approximately equal amounts of nitrate and nitrite were obtained here (Fig.4.1.1.4). Mead et al. [1976] obtained much more nitrite than nitrate (22 vs. 6), while Tiehm [1999] obtained more nitrate (42 vs. 4). These discrepancies can be explained on the basis of the results presented by Petrier et al. [1999]. Mead et al., [1976] give the initial rates of formation, with data from less than 10 min of irradiation; here the rates are obtained averaged over a 20 min experiment. Tiehm [1999] obtained rates averaged over a 60 min run. It is evident from Petrier et al. [1999] that the nitrate/nitrite ratio increases with time. Thus the above observations are consistent with each other.

4.1.3. Nitrate and Nitrite as Function of Gas Composition

Figure 4.1.3.1 shows the rate of formation of NO_3^-, NO_x^- ions and the Zeldovich predictions as function of the nitrogen/oxygen gas composition.

The maximum rate of nitrate and nitrite formation was obtained at a gas mol fraction of 0.6 nitrogen. The rate of formation of nitrite and nitrate in the absence of external oxygen gas is below the detection limit. This suggests that oxygen from water is not involved in the nitrite and nitrate formation under sonication.

It should be noted that the gas composition in the cavities may differ somewhat from that in the sparging gas. A gas diffuses into the cavity during the expansion phase, then if there is a difference in the solubilities of the gases (section 2.2), then there can be a difference in the composition of the gas in the cavitation bubble and the sparging gas. As O_2 is slightly more soluble than N_2 [$X(O_2)= 1.75 \times 10^{-5}$, $X(N_2)= 1.70 \times 10^{-5}$ at 278 K], the gas in the cavities would be expected to have a composition somewhat < 0.6 mol fraction N_2.

It is thus necessary to have molecular oxygen in the system in order to obtain a significant rate of reaction. From a kinetic viewpoint, the dissociation of O_2 is thus a major initial step. This agrees with the mechanism suggested for combustion of stoichiometric fuel-air mixtures in engines (the Zeldovich mechanism) (section 2.4). The resulting kinetic analysis suggests that the rate of formation of NO is proportional to the product of the N_2 concentration and the square root of the O_2 concentration. The dependence suggested by Zeldovich equation is shown in Figure 4.1.3.1. However, it is not spectacularly successful in explaining the dependence on the sparging gas composition.

4.1.4. Nitrate and Nitrite as Function of Time

The variation of the rate of formation of NO_x^- with time was done with gas 0.6 mol fraction of nitrogen and 900 kHz of ultrasound at 5°C. The results are presented in figure 4.1.4.1. Each data point represents the average of three determinations.

The graph suggests that the rate of NO_x^- formation increases after 60 minutes of sonication. The amount of nitrite increases, and then decreases with increasing time of sonication. This is due to more oxidation of nitrite to nitrate by the hydrogen peroxide formed from

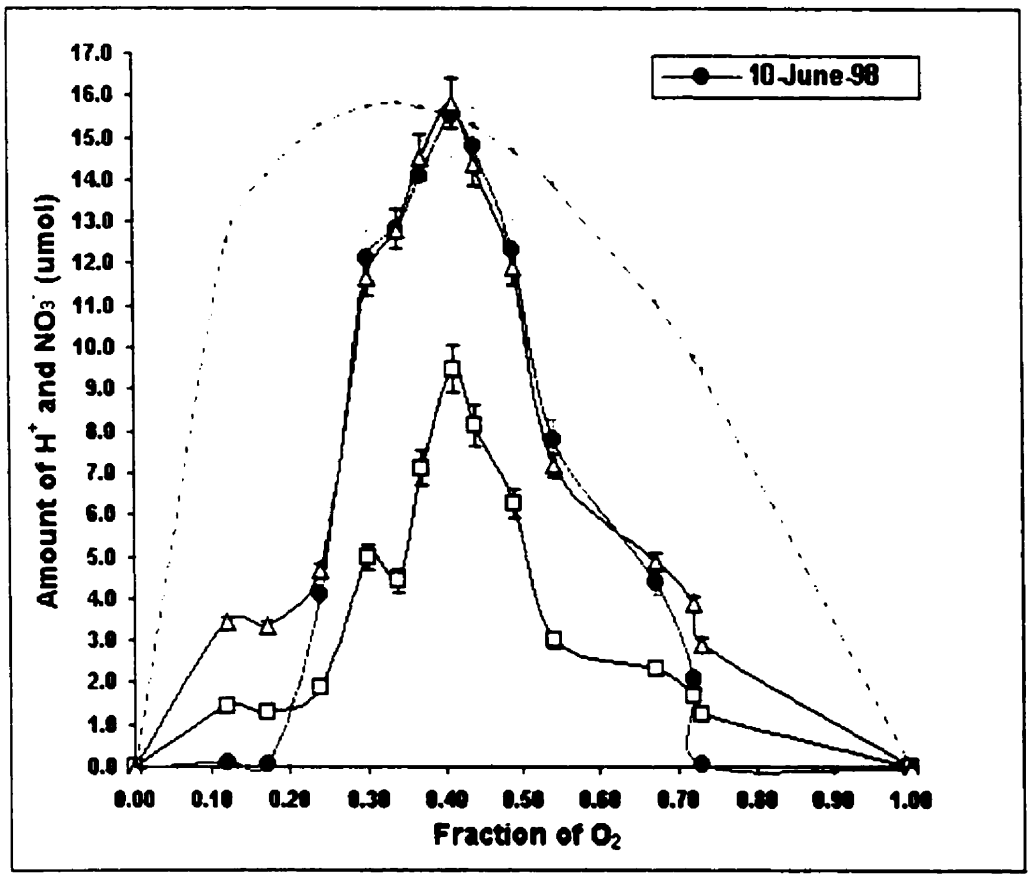

Fig.4.1.3.1. The variation of the amount of the hydrogen and nitrate ions with gas composition at 5°C. Hydrogen ions (•), nitrate alone (□), total nitrite plus nitrate (Δ) and the predictions of the Zeldovich equation (...). 20 min irradiation, 900 kHz (27 W) ultrasound.

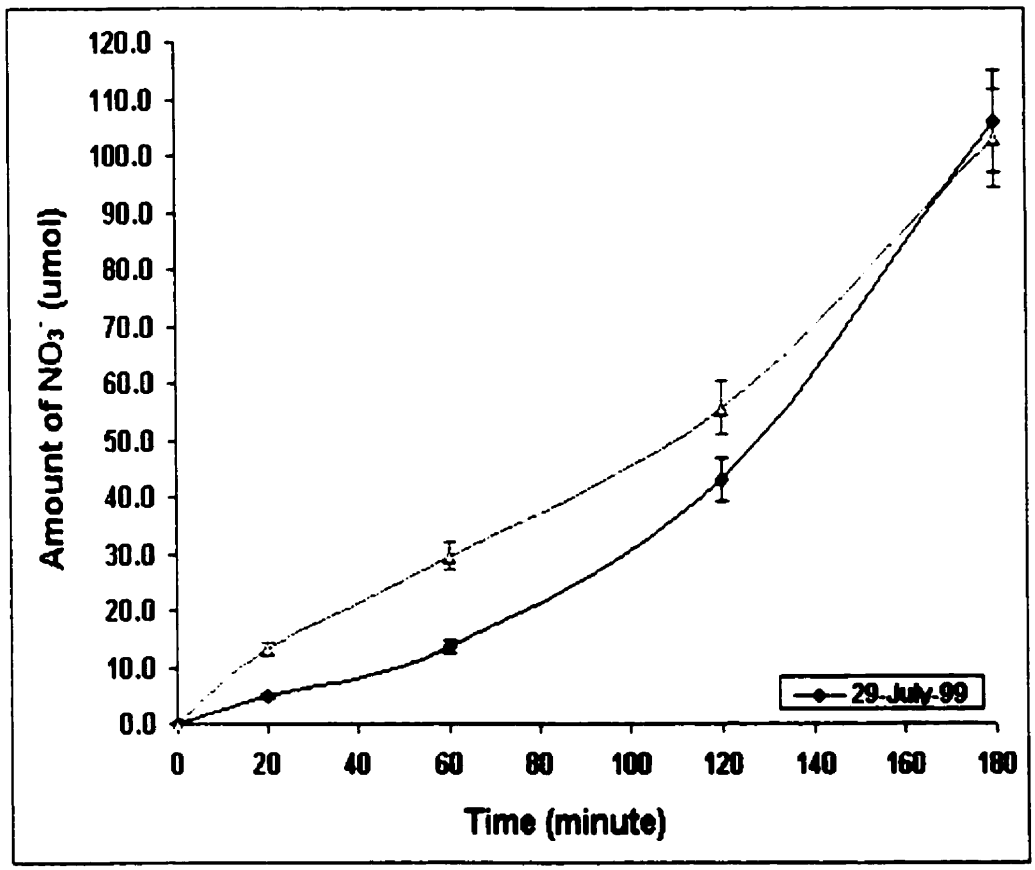

Figure 4.1.4.1. The variation of the amount of the nitrate ions with time at 5°C. The nitrate alone (♦) and total nitrite plus nitrate (Δ), 900 kHz (52 W) ultrasound. The amount of nitrite is given by the difference in the two curves, and reach a maximum at about 60 min.

sonication of water (section 1.1). This agrees with the previous work of Petrier, et al. [1999].

4.1.5. Nitrate and Nitrite as Function of Temperature

The variation of rate of NO_x^- with temperature was done at gas mol fraction 0.6 nitrogen with 900 kHz of ultrasound for 20 minutes. The results are presented in figure 4.1.5.1. Each point again represents the average of three determinations.

The graph shows that the rate decreases as temperature of bulk solution increases. As bulk temperature increases, the vapour pressure of water increases, the collapse of the cavity is cushioned more, and the "hot spot" temperature decreases. This trend agrees with section 2.3.2.4 and equation (2.4.4), i.e. kinetics and thermodynamics of $NO_{(g)}$ formation are both unfavourable as the temperature of the collapsing cavitation bubbles decreases with increasing bulk temperature.

It is possible to try to explain the results on the basis of kinetics. Suggested values of rate constants for the steps that could be involved can be found [Heywood, 1988]. This includes rates for fundamental steps such as the decomposition of water [Hart and Henglein, 1986]. However, if the effective temperature in the imploding cavity reaches values of order of 5000 K [Suslick, 1990], and if the pressures are well above an atmosphere, then it is likely that equilibrium considerations will be more significant. At such high temperatures and pressures the rates of reaction are so great that thermodynamic equilibrium states can be reached quite quickly.

The predicted equilibrium concentrations of NO and $OH^\bullet$ radicals in particular are surprisingly large at 5000 K, as seen in tables 2.3.2.4 and 2.3.2.6. It is thus quite likely that subsequent reactions between NO and NO_2 and $OH^\bullet$ can take place in the imploding cavity.

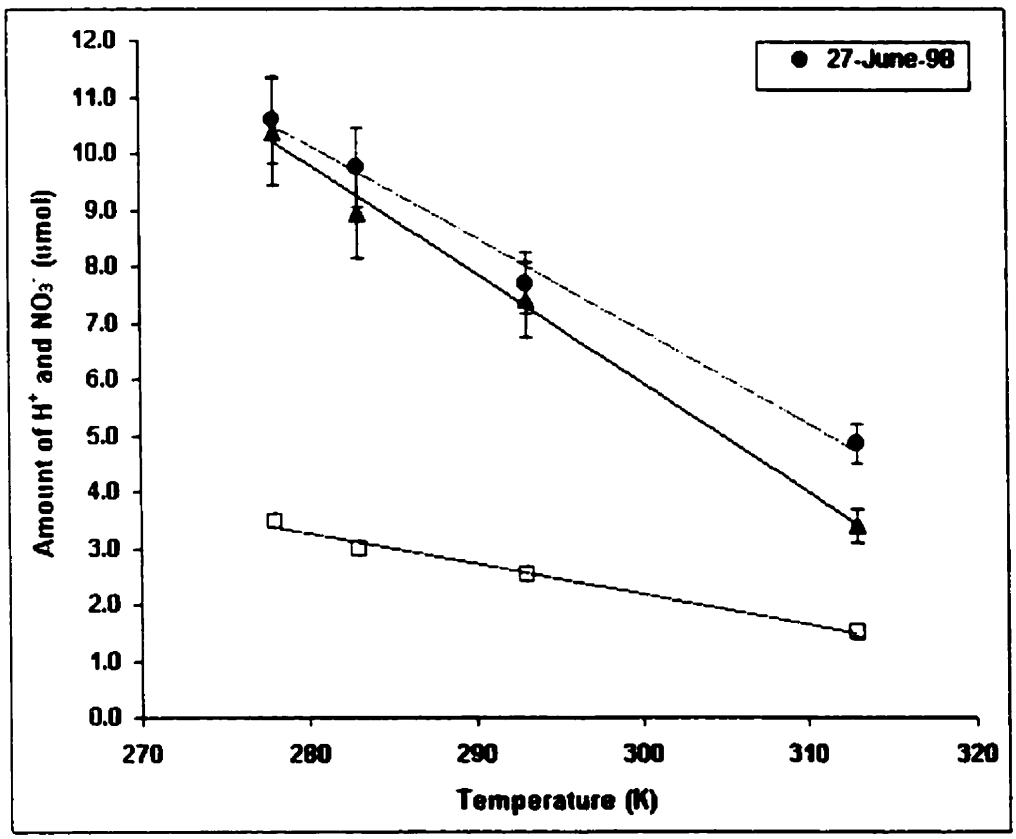

Figure 4.1.5.1. The variation of the amount of the hydrogen and nitrate ions with temperature. Hydrogen ions (•), nitrate alone (□) and total nitrite plus nitrate (Δ), 20 min of irradiation, 900 kHz (27 W) ultrasound. The lines are best fits to a linear dependence.

The solubility of NO and NO_2 in water is surprisingly small [Lee, 1984]; this is why it is not easy to make nitric acid industrially by dissolving NO_x gas in water. As in the case of atmospheric chemistry [Seinfeld and Pandis, 1998], it is thus likely that the following three-body reactions occur in the gas phase (M is a "third body"):

$$NO + OH^{\bullet} + M \rightarrow HNO_2 + M, \text{ and}$$

$$OH^{\bullet} + NO_2 + \rightarrow HNO_3 + M$$

The products would then dissolve in the surrounding water and dissociate to form NO_2^- and NO_3^- ions.

The temperature dependence of the rates (Fig. 4.1.5.1) supports this suggestion, as reactions in the gas phase of the imploding cavity should be favoured by a lower bulk temperature. The lower vapour pressure of the water at a lower bulk temperature results in a more energetic cavity implosion and a higher "hot spot" temperature [Entezari et al., 1997].

As seen in tables 2.3.2.4 and 2.3.2.5, there is much less NO_2 than NO expected from the equilibrium calculations; it would be expected that initially there is more NO_2^- formed. This can, however, subsequently react with hydrogen peroxide to give NO_3^-; this is the process we used to convert nitrite to nitrate for total fixed nitrogen determinations. As indicated in Reference [Virtanen and Ellfolk, 1950], this conversion seems to be favoured at lower pH values, and the pH decreases with time of sonication. This suggests that it occurs in the aqueous phase rather than in the imploding cavity.

4.1.6. Nitrite and Nitrate Formation in KCl as Function of Time

The variation of the amount of NO_x^- in KCl (2.28 M) was done at gas mol fraction 0.6 nitrogen with 900 kHz (52 W) of ultrasound at 5°C. The results are presented in figure

4.1.6.1 and 4.1.6.2. Most of points in these figures represent the average of three determinations.

The graph shows that the amount of NO_3^- increases reasonably linearly. There is no evidence of NO_2^- being oxidized to NO_3^- as time progresses, as suggested in Figure 4.1.4.1. This may be because the presence ions (KCl) attenuates the oxidation of nitrite to nitrate.

The presence of ions in the solution also increases the total nitrate formation about 10 fold. This agrees with the previous research of Wakeford, et al., 1999.

A possible explanation for the higher rate of NO_x^- in the presence of ions in the solution is as follows:

The cavitation threshold, P_A, is the minimum negative pressure needed to form a cavity in a liquid in a rarefaction condition. The presence of ions in the solution should lead to an increase in the cavitation threshold. This is due to the strong interionic forces in solutions of high ionic strength, viscosity and/or surface tension. The increase in cavitation threshold should increase the intensity of cavitation collapse as the maximum pressure, P_M, increases.

$P_M = P_h + P_A$, where P_h, is the hydrostatic pressure within liquid.

This, in turn, will enhance the sonochemical reaction. Indeed, these phenomena have been reported by Jarman and Taylor (1965). They reported an increase in the sonoluminescence emitted from liquids with a relatively high surface tension and viscosity.

The attenuation of nitrite oxidation to nitrate in KCl solution may be caused by the decrease of hydrogen peroxide formation. The chloride ions present will react with hydroxyl radicals based on the following reaction [Spinks and Woods, 1990]:

$$OH^{\bullet} + 2Cl^- \rightarrow OH^- + Cl_2^{\bullet -} \qquad (4.1.6.1)$$

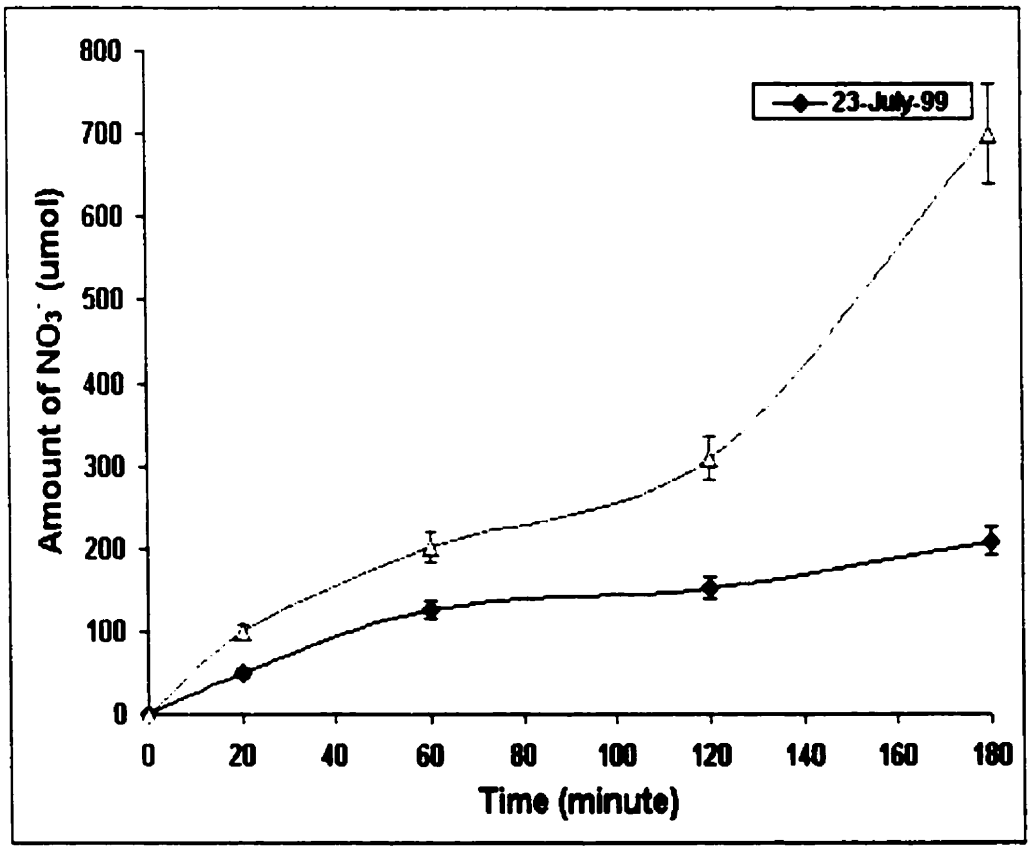

Figure 4.1.6.1. The variation of the amount of the nitrate ions in KCl (1.14 M) with time at 5°C. The nitrate alone (♦) and total nitrite plus nitrate (Δ), 900 kHz (52 W) ultrasound.

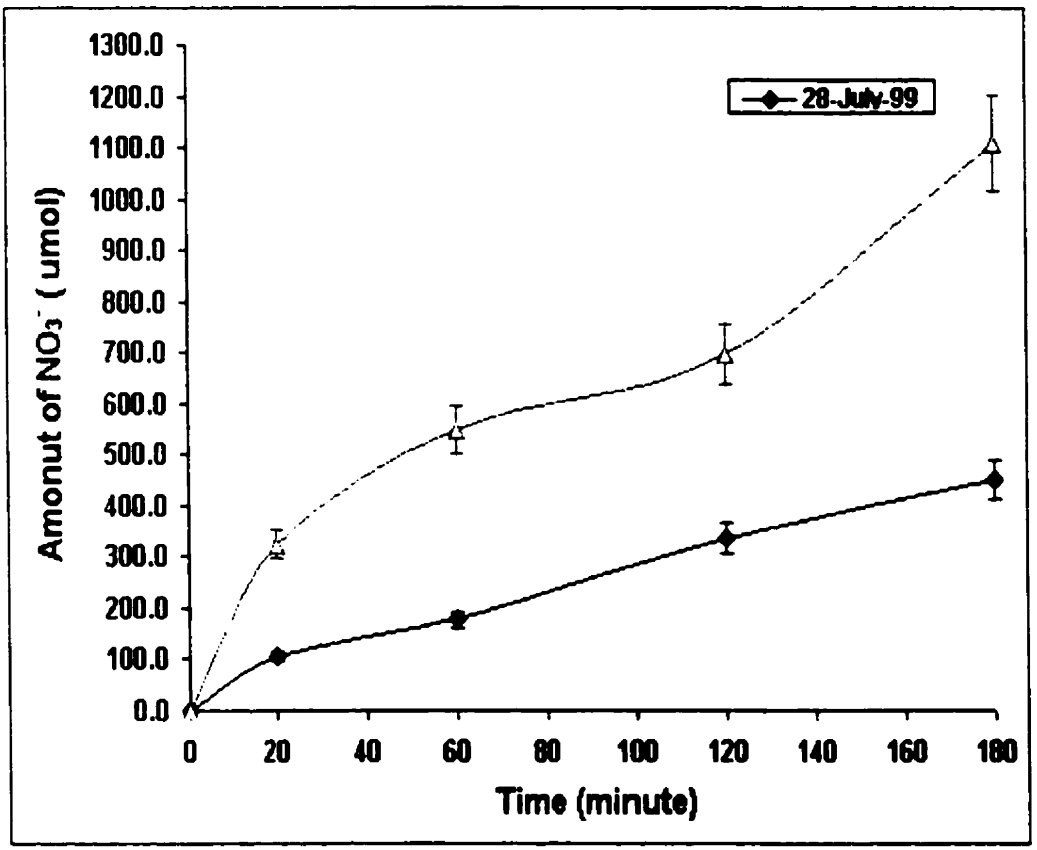

Figure 4.1.6.2. The variation of the amount of the nitrate ions in KCl (2.28 M) with time at 5°C. The nitrate alone (♦) and total nitrite plus nitrate (Δ), 900 kHz (52 W) ultrasound.

It consists the following steps:

$$OH^{\bullet} + Cl^{-} \rightarrow ClOH^{\bullet -}, k = 4.3 \times 10^{9} \text{ L mol}^{-1} \text{ s}^{-1}. \quad (4.1.6.2)$$

$$ClOH^{\bullet -} + H^{+} \rightarrow Cl^{\bullet} + H_2O, k = 2.1 \times 10^{10} \text{ L mol}^{-1} \text{ s}^{-1}. \quad (4.1.6.3)$$

$$Cl^{\bullet} + Cl^{-} \rightarrow Cl_2^{\bullet -}, k = 2.1 \times 10^{10} \text{ L mol}^{-1} \text{ s}^{-1}. \quad (4.1.6.4)$$

These reactions will lower the amount of hydroxyl radicals in the solution that eventually produce hydrogen peroxide that oxidizes nitrite to nitrate (see Appendix B.3).

4.2. Mixture of N_2 and H_2 in water

4.2.1. Reproducibility

4.2.1.1. Ammonia Calculation from pH

Figure 4.2.1.1 shows the rate of formation of total ammonia (NH_3 and NH_4^+) as calculated from pH as a function of nitrogen/hydrogen gas composition (see Appendix C.1). Three independent determinations are shown, together with the mean. Studies were done for 20 min with 52 W of 900 kHz ultrasound at 5°C. The experiment was done in triplicate.

In 4.1, there was good equivalence between H^+ and NO_x^- concentration. However, as ammonia is a weak base, OH^- can not be equated to NH_4^+ (see Appendix C.1).

4.2.1.2. Ammonia Calculation and Ammonia from Nessler's Reagent

Figure 4.2.1.2 shows the rate of ammonia calculated from pH and ammonia determined by Nessler's Reagent as a function of nitrogen/hydrogen gas composition. Three independent determinations are shown, together with the mean. Studies were done for 90 min with 80 W of 850 kHz ultrasound at 5°C. The experiment was done in triplicate.

The graph shows that the two methods for determination of total ammonia match reasonably well. Nessler's reagent was subsequently primarily used to determine ammonia formed in the 850 kHz reactor. The pH of the solutions was very sensitive to impurities, e.g. oxides formed on the brass.

4.2.1.3. Ammonia with Different Ultrasonic Equipment

Figure 4.2.1.3 shows the rate of calculated ammonia from pH as a function of nitrogen/hydrogen gases, obtained with the 900 kHz and 850 kHz reactors. Three

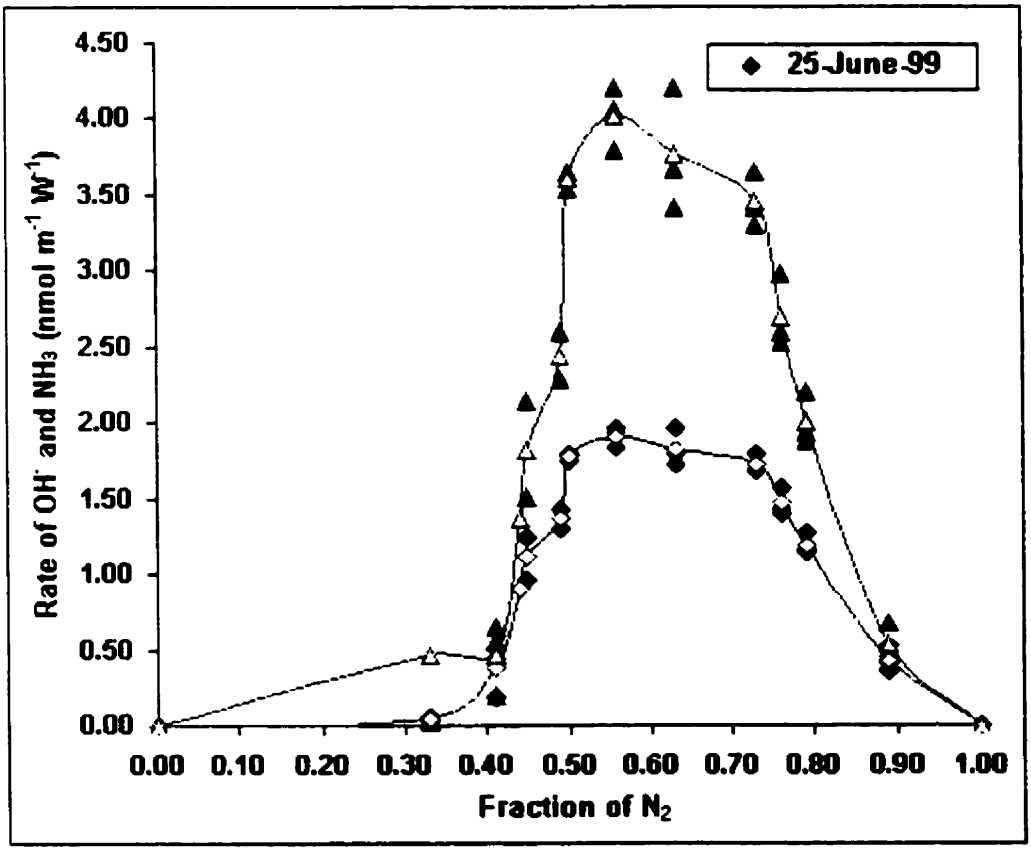

Figure 4.2.1.1. Calculation of the rate of ammonia from pH as a function of composition of N_2 and H_2 mixture with power 52 W, 900 kHz irradiation at 5°C. Ammonia calculation (▲ individual data, Δ mean) and hydroxide ions (♦individual data, ◊ mean).

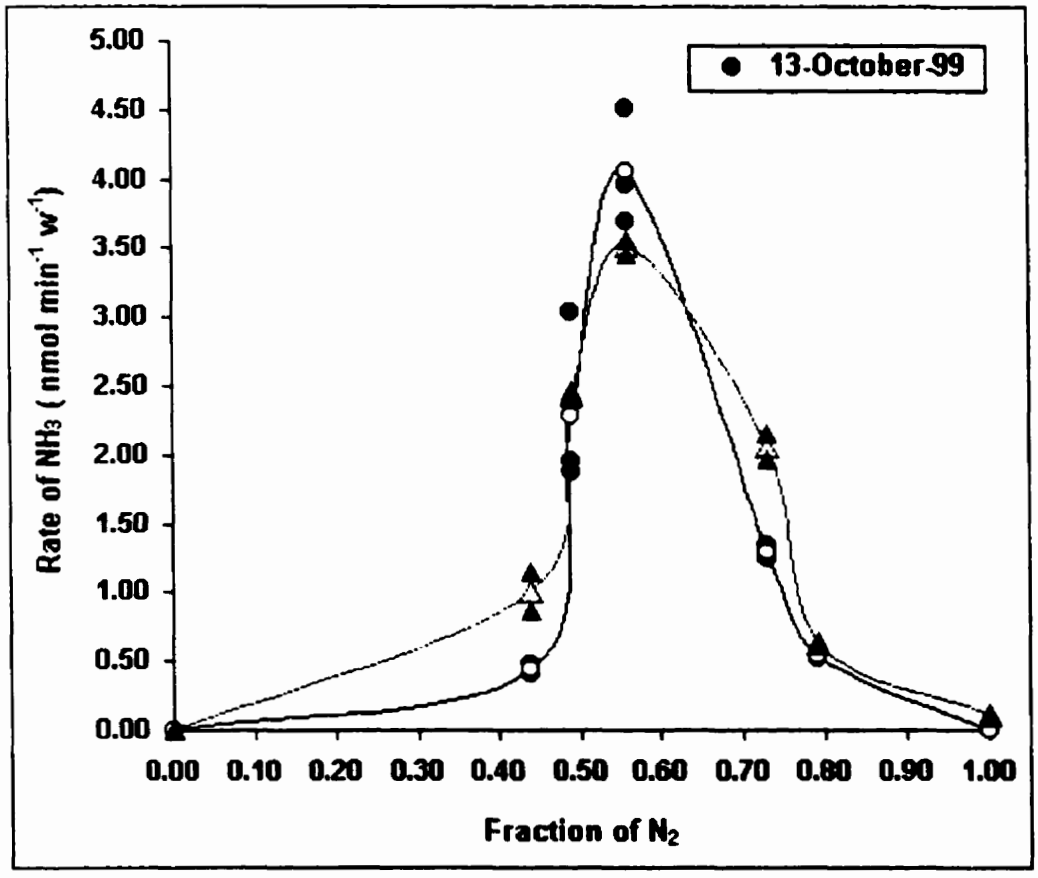

Figure 4.2.1.2. Reproducibility of the rate of ammonia calculation from pH with ammonia from Nessler's reagent as a function of composition of N_2 and H_2 mixture with power 80 W, 850 kHz irradiation at 5°C. Ammonia calculation (▲ individual data, Δ mean) and ammonia from Nessler's reagent (• individual data, o mean).

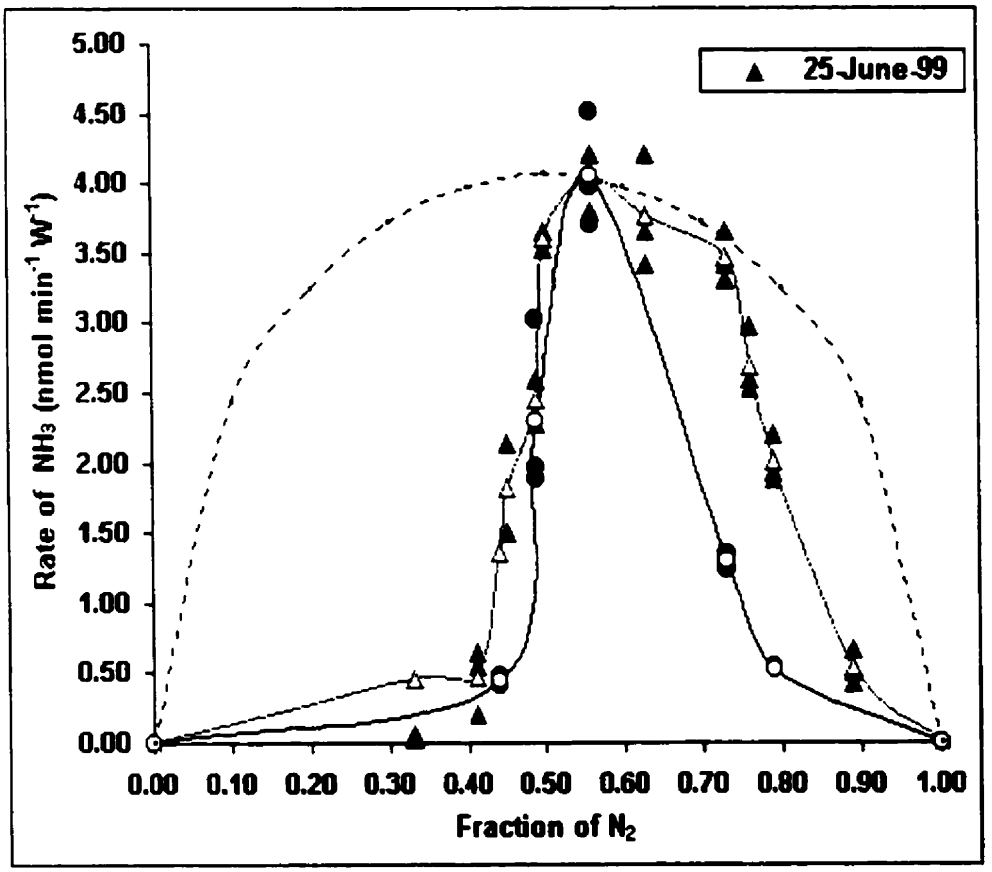

Figure 4.2.1.3. Reproducibility of the rate of ammonia with power 52 W, 900 kHz, 100 mL water and 80 W, 850 kHz, 382 mL water. Ammonia calculated from pH with 900 kHz (▲ individual data, Δ mean) and ammonia calculated from pH with 850 kHz (• individual data, o mean). Gas concentration dependence predicted by (4.2.2.2.12) (---).

independent determinations are shown, together with the mean. Studies were done for the following cases at 5°C: 20 min, 52 W of 900 kHz ultrasound, 100 mL, and 90 min, 80 W of 850 kHz ultrasound, 382 mL. The sparging gas was in both cases a mixture of 0.6 N_2, 0.4 H_2 at 2.9 mL s^{-1}.

The graph shows that the rate of ammonia formation obtained from the two reactors matched very well. This is important, as the reactors were geometrically quite different (section 3.2.6 and 3.2.7), and as different volumes of water were used.

Based on the data presented in section 4.2.1, it can be seen that the rate of formation of ammonia is nearly 10 times less than that of NO_x^- (section 4.1.1). The reproducibility in the case of ammonia formation is somewhat poorer than the ± 10% estimated for NO_x^- (see section 4.1.1.4). Results obtained from pH measurements were at times erratic; these were rejected and not shown here. This was presumably due to contamination with metallic compounds cleaned off the walls of the 850 kHz reactor.

4.2.2. Ammonia as Function of Gas Composition

4.2.2.1. Experimental Results

The variation of the rate of ammonia formation with gas composition of N_2/ H_2 mixture is shown in Figure 4.2.1.3. The experiments were done at 5° C with using 900 and 850 kHz ultrasound. The ammonia concentrations were determined by pH measurements and Nessler's reagent.

The maximum rate of ammonia formation was obtained at a gas mol fraction of 0.6 nitrogen. The data obtained from both reactors using both analytical techniques agreed

well at that composition.

The solubilites of N_2 and H_2 in water at 278 K are $X(N_2) = 1.70 \times 10^{-5}$ and $X(H_2) = 1.70 \times 10^{-5}$ according to (2.2.1) and (2.2.3). Thus the gas in the cavities would be expected to also be at 0.6 mol fraction N_2.

Figure 4.2.1.2 also shows traces of ammonia formed without the presence of external hydrogen gas. Hydrogen atoms are produced from water during sonication (section 1.1), so that this is not unexpected. This result agrees with previous work by Sokol'skaya and El'piner [1957].

Data shown in figure 4.2.1.1, however, did not show detectable traces ammonia formation in the absence of external hydrogen gas. A possible explanation is that the acidification through dissolving of residual CO_2 is greater than the effect of ammonia. The pH measurement of the solution with no H_2 indicated an acidic rather than basic solution.

This result suggests that the presence of external hydrogen gas in the solution is nevertheless needed to produce a significant amount of ammonia.

4.2.2.2. Possible Kinetic Mechanism

A simple possible mechanism of ammonia formation can be derived as follow:

$$H_2 \overset{1}{\rightleftarrows} H^\bullet + H^\bullet ; \qquad K_1 = (H^\bullet)^2 / H_2 \text{ , at equlibrium} \qquad (4.2.2.2.1)$$

$$N_2 \overset{2}{\rightleftarrows} N^\bullet + N^\bullet ; \qquad K_2 = (N^\bullet)^2 / N_2 \text{ , at equlibrium} \qquad (4.2.2.2.2)$$

$$N^\bullet + H^\bullet \overset{3}{\rightleftarrows} NH \qquad (4.2.2.2.3)$$

$$NH + H_2 \overset{4}{\rightleftarrows} NH_3 \qquad (4.2.2.2.4)$$

It is reasonable to assume that N_2, H_2 >> $N^\bullet$, $H^\bullet$, NH, NH_3. Third bodies for reactions such as 4.2.2.2.3 are ignored, as a high pressure is always present. It is also assumed that N_2 and H_2 are constant, that $H^\bullet$ from water is negligible and that $H^\bullet$, $N^\bullet$, and NH concentrations are in a stationary state. The differential rate equations are then:

$$(dH/dt) = 2k_1(H_2) - k_3(N^\bullet)(H^\bullet) - 2k_{-1}(H^\bullet)(H^\bullet) = 0 \qquad (4.2.2.2.5)$$

$$(dN/dt) = 2k_2(N_2) - k_3(N^\bullet)(H^\bullet) - 2k_{-2}(N^\bullet)(N^\bullet) = 0 \qquad (4.2.2.2.6)$$

$$(dNH/dt) = k_3(N^\bullet)(H^\bullet) - k_4(NH)(H_2) = 0 \qquad (4.2.2.2.7)$$

$$(dNH_3/dt) = k_4(NH)(H_2) \qquad (4.2.2.2.8)$$

If we further assume that

$(H^\bullet) = [K_1(H_2)]^{0.5}$ and $(N^\bullet) = [K_2(N_2)]^{0.5}$, i.e. rate of (4.2.2.2.3) << (4.2.2.2.1) and (4.2.2.2.2), then equation (4.2.2.2.7) gives

$$k_3(N^\bullet)(H^\bullet) - k_4(NH)(H_2) = 0 \qquad (4.2.2.2.9)$$

$$(NH) = k_3(N^\bullet)(H^\bullet) / k_4(H_2) = k_3[K_1(H_2)]^{0.5}\,[K_2(N_2)]^{0.5} / [k_4(H_2)] \qquad (4.2.2.2.10)$$

$$(dNH_3/dt) = k_4(NH)(H_2) = k_4(H_2)k_3[K_1(H_2)]^{0.5}\,[K_2(N_2)]^{0.5} / [k_4(H_2)] \qquad (4.2.2.2.11)$$

$$\text{Thus, } (dNH_3/dt) = k_3[K_1 K_2]^{0.5}\, p^{0.5}(H_2)\, p^{0.5}(N_2) \qquad (4.2.2.2.12)$$

The calculations from equation (4.2.2.2.12) give the maximum rate at gas mol fraction 0.5 nitrogen. Figure 4.2.1.3 shows a comparison between the experimental results the calculated data from this simple mechanism.

A questionable simplification for the mechanism is to assume $(N^\bullet) = [k_2(N_2)]^{0.5}$. The equilibrium calculations in section 2.3.2 suggest that $(H^\bullet)$ >> $(N^\bullet)$. Thus the rate of 4.2.2.2.3 should not be neglected as compared to the rate of the reverse reaction in 4.2.2.2.2. Removal of this assumption makes it impossible to obtain a simple mathematical form for the overall

rate. It suggests, however, that there should be a bias in the overall rate towards N_2 concentrations, in agreement with experiment.

4.2.3. Rate of Ammonia Formation

The highest rate obtained of ammonia formation in this study can be seen in Figure 4.2.1.3 to be 4.2 x 10^{-9} mol min^{-1} W^{-1}. This is equivalent to 1.6 x 10^{-2} μg W^{-1} mL^{-1} min^{-1} cm^2. About 3 times larger than the results of the only other investigator [Sokol'skaya and El'piner, 1957]: 5.0 x 10^{-3} μg W^{-1} mL^{-1} min^{-1} cm^2. A higher rate our experiments can be due to the use of an optimum nitrogen/hydrogen mixture and a lower temperature.

4.2.4. Ammonia as Function of Time

The variation of the amount of ammonia with time was done at gas mol fraction 0.6 nitrogen with 900 kHz (52 W) of ultrasound at 5°C. The results are presented in figure 4.2.4.1. Most of points in these figures represent the average of three determinations.

The graph shows that the amount of ammonia increases quite linearly.

4.2.5. Ammonia Formation as Function of Temperature

The variation of the rate of ammonia formation with temperature is shown in Figure 4.2.5.1. The data were taken after 20 minutes exposure to 900 kHz ultrasound with sparging gas 0.6 mol fraction of nitrogen. The ammonia concentrations were determined by pH. Each data point represents the mean of three experiments.

The rate of ammonia formation decreases as the temperature of bulk solution increases. This shows that kinetics – not equilibrium – is the dominant consideration for

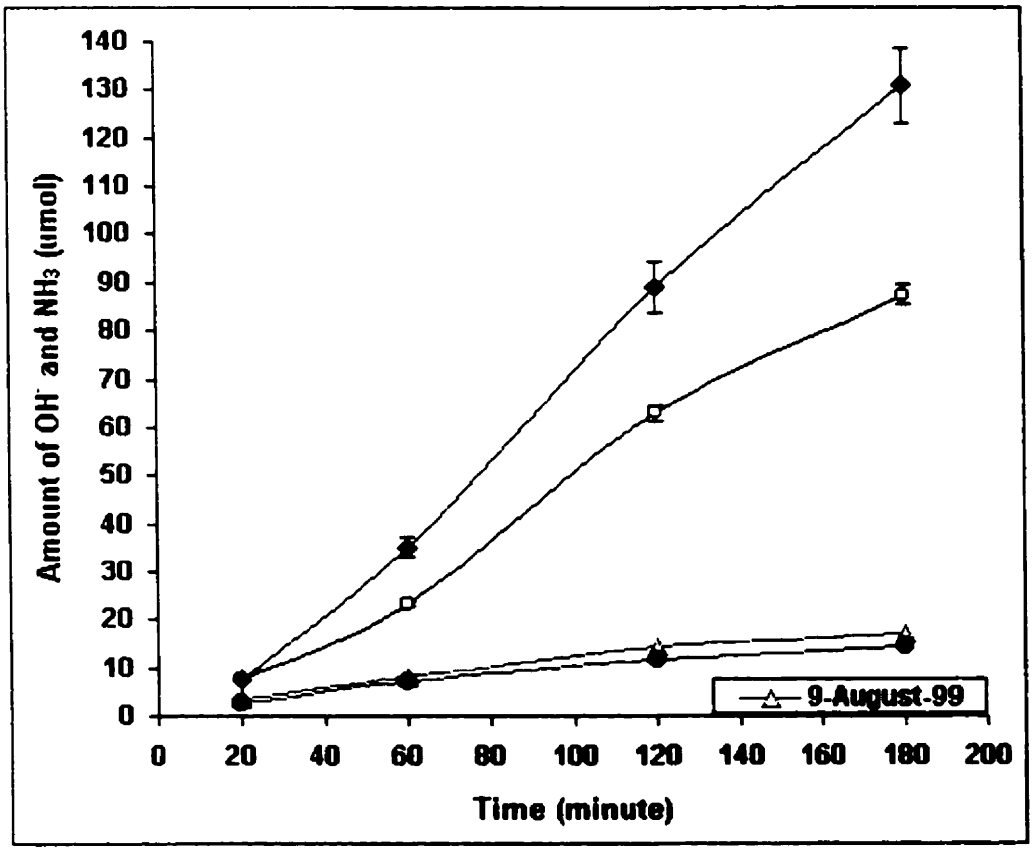

Figure 4.2.4.1. The variation of the amount of hydroxide ions and calculated ammonia with time at 5°C. Ammonia in water (♦), ammonia in KCl (1.0 M) (O), Hydroxide ions in KCl (1.0 M) (Δ), hydroxide ions in water (•), 900 kHz (52 W) ultrasound.

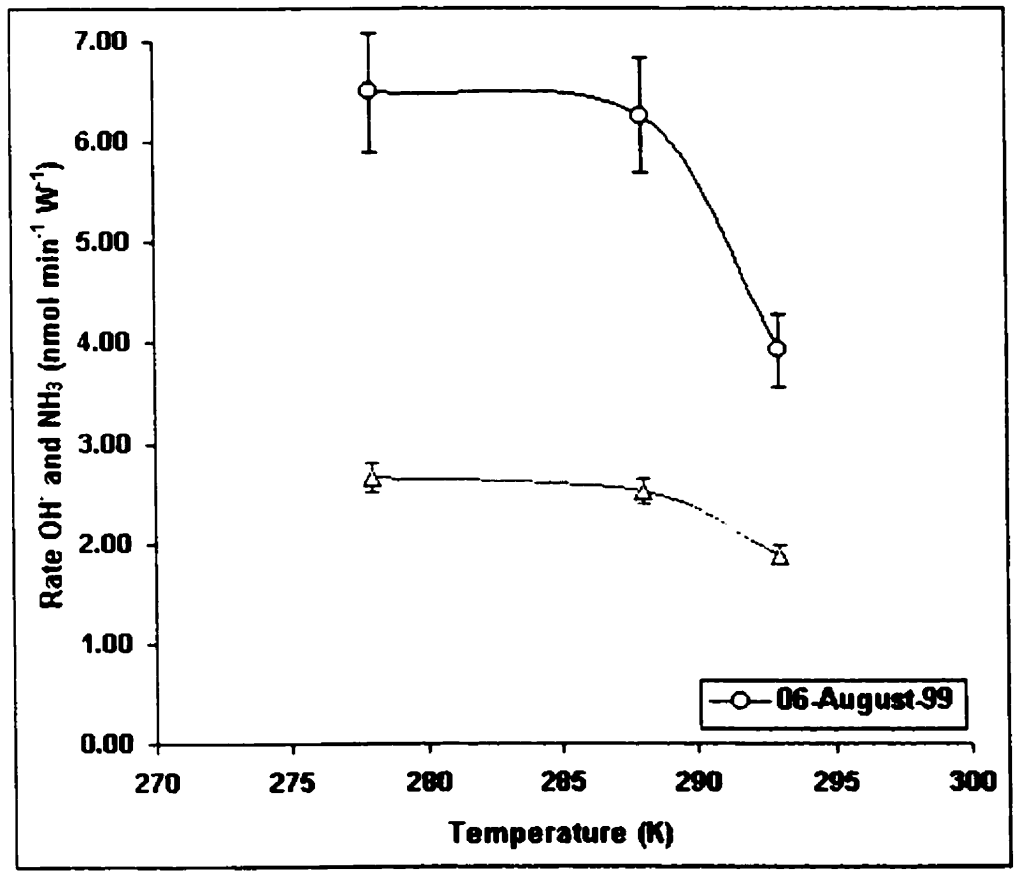

Figure 4.2.5.1 The variation of the rate of hydrogen ions and calculated ammonia with temperature. Ammonia (O), hydroxide ions (Δ) 20 min of irradiation, 900 kHz (52 W) ultrasound.

synthesizing ammonia in these experiments. The equilibrium is less favourable at high "hot spot", low bulk temperatures (section 2.3.2.3).

4.2.6. Effect of Ionic Strength on Production of Ammonia

The variation of the amount of ammonia in KCl (1.0 M) with time is shown in Figure 4.2.4.1. The experiment was done at 5°C with 900 kHz ultrasound and for gas with 0.6 mol fraction of nitrogen.

The calculated ammonia was determined by pH. Each data point represents the mean of three determinations.

The graph shows that the presence of ions decreases the rate of ammonia formation by about 40 %. This is the opposite effect to nitrate formation, where the presence of ions increased the rate by 10 fold (section 4.1.6).

4.3. Ammonia Formation in Octane

The sonochemistry of nitrogen/hydrogen gas mixtures in water shows the formation of ammonia. Varying conditions such as temperature and the presence of ions were considered as means for potential increase in the rate of ammonia formation. Section 4.2.5 shows that the presence of ions in water does not increase the rate, in contrast to the case of nitrate formation, the rate can be increased 10 fold by the introduction of ions.

The use of the catalyst usually used in the "Haber-Bosch" process may increase the sonochemical formation of ammonia significantly. This catalyst, however, can not be used in water as an explosive reaction occurs. Other liquids should thus be used as a medium for catalyst.

Octane was used for this experiment because at 25°C it has vapour pressure similar to water at 5°C [HCP, 1999]. Alkanes are also relatively inert to the effect of ultrasound, in contrast to aromatic compounds, which form a char [Kruus et al., 1987; Mizukoshi et al., 1999]. With these properties, the conditions usually used in water can be applied for octane.

4.3.1. Ammonia Formation in Octane as Function of Temperature

The variation of the total amount of ammonia in octane with temperature is shown in Figure 4.3.1.1. The experiment was done for 180 minutes with using 850 kHz of ultrasound and for 0.6 mol fraction of nitrogen gas. The ammonia concentrations were determined by Nessler's reagent. Each data point represents two independent experiments.

It was expected that most of the ammonia would be flushed out as a gas and be trapped by a 100 mL of HCl (1.0×10^{-5} M) (section 3.3.4). The solubility of ammonia in octane is less than in water (section 2.2).

In these 180 min runs, the total amount of ammonia formed was less than in water ($\approx$ 10%). Ammonia was obtained both in the dilute acid through which the exiting gases passed, as well as in the octane. Since the solubility of ammonia in alkanes is substantial (see 2.2), some ammonia was found in the octane. At 25°C, the ammonia found in the octane was 38% and 62% in exiting gas. If the total amount of ammonia formed were greater, then the proportion trapped in the dilute acid would be greater.

A Preliminary GC-MS analysis was carried out to detect possible impurities formed from sonochemical destruction of octane. The GC-MS spectra of reused octane did not show any such impurities.

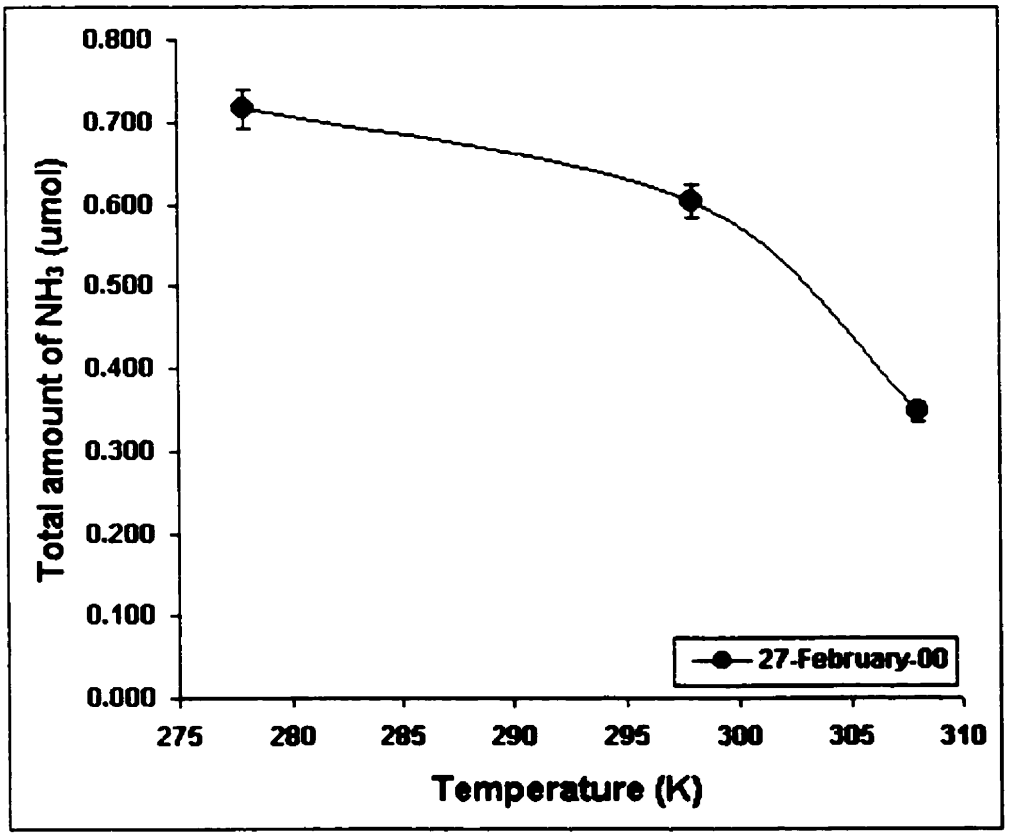

Figure 4.3.1.1. The variation of the total amount of ammonia in the fresh octane with temperature. 180 min of irradiation, 850 kHz (80 W) ultrasound.

The graph shows that the ammonia formation in octane decreased with increasing temperature of bulk solution. This trend again shows the kinetics – not equilibrium – is the dominant consideration for synthesizing ammonia sonochemically in any liquid medium.

The octane was reused, after extraction of ammonia from it. The residual water in the octane used was reduced by mixing in some sodium sulphate and letting it settle for at least 10 hours.

4.3.2. Effect of a Catalyst on Ammonia Formation

The variation of the total amount of ammonia in octane under different conditions is shown in figure 4.3.2.1. The experiment was done for 180 minutes at 25° C with 850 kHz of ultrasounds and for 0.6 mol fraction of nitrogen gas. The ammonia concentration was determined by Nessler's reagent. Each data point represents two independent experiments. The amount of ammonia formed in these experiments with reused octane was only about 50% of that using fresh octane (Fig. 4.3.1.1).

The graph shows that the presence of the "Haber-Bosch" catalyst does not increase the ammonia formation significantly. This may be due to inactivity of this catalyst in the presence of alkanes, the need to reactivate the catalyst before use, or a poor choice of physical conditions and reactor geometry.

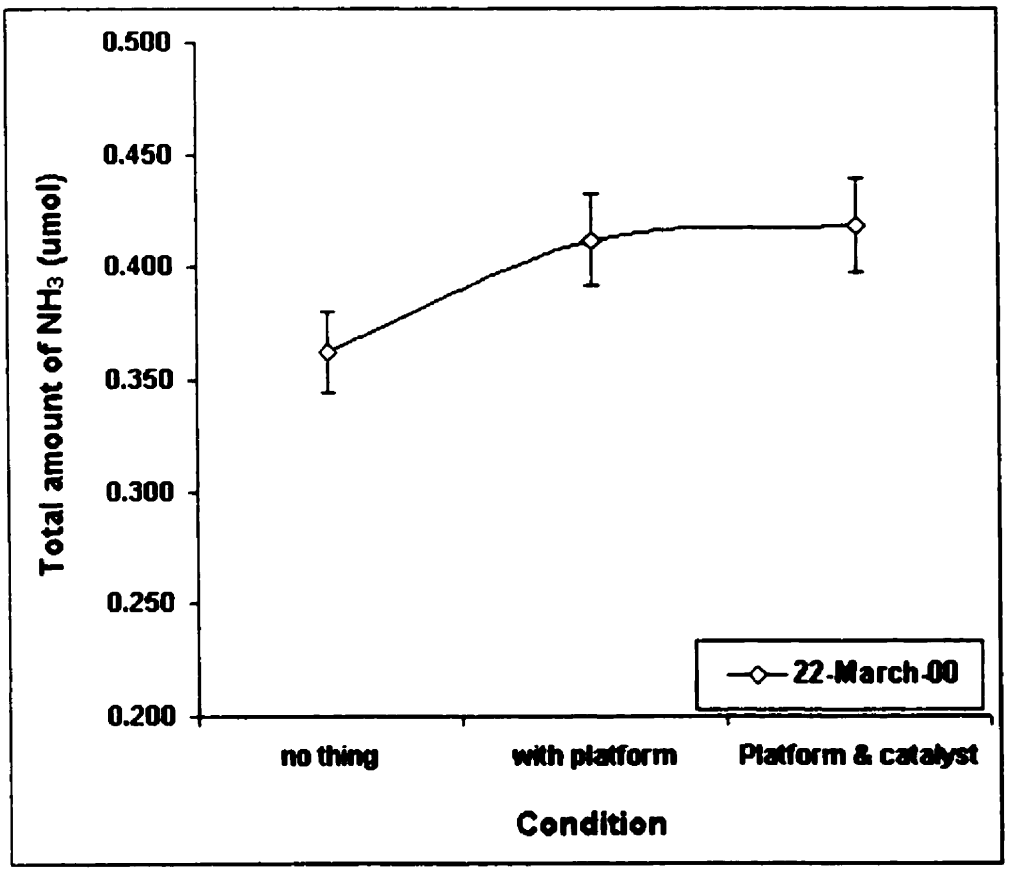

Figure 4.3.2.1. The variation of the total amount of ammonia in the reused octane under different conditions at 25°C. 180 min of irradiation, 850 kHz (80 W) ultrasound.

Conclusions

At ambient conditions, nitrite, nitrate and ammonia can be synthesized from their elements in a liquid medium by sonochemistry.

5.1. Nitrite and Nitrate

The maximum rate of NO_x^{-1} is obtained at a gas mol fraction of 0.6 nitrogen and at a lower temperature (278 K). The absolute rates (nmol min^{-1} W^{-1}) of formation of NOx^{-1} found here agree well with data from previous similar studies. The differences in the NO_2^-/NO_3^- ratio found among various studies can be satisfactorily explained though a mechanism where HNO_2 and HNO_3 are formed in the gas phase of the imploding cavity, and then dissolve in the water and dissociate to ions. The NO_2^- species is initially substantially favoured, as considerably more NO is formed than NO_2. The NO_2^- is subsequently oxidized to NO_3^- by the H_2O_2 formed.

Thermodynamic calculations indicate that at the "hot spot" temperature of about 5000 K believed to be present, the formation of NO and NO_2 is expected. At such high temperatures, thermodynamics would provide a good approximation of the actual situation, since the rates of reactions would be very rapid.

The reaction needs O_2 in order to proceed to a significant degree; no NO_x^- was detected in the absence of oxygen gas. The investigation of the dependence of NO_x^- formation on gas composition is the most important novel contribution of the NO_x^- experiment.

The presence of ions (KCl) in the solution can increase the yield of nitrate formation. KCl (2.28 M) can increase nitrate formation 10 fold.

5.2. Ammonia

The maximum rate of ammonia formation in water is obtained at a gas mol fraction of 0.6 nitrogen and at a lower temperature (278 K). The absolute rate (nmol min^{-1} W^{-1}) of formation of ammonia found here is 3 times higher than data from the only previous similar study, probably a better gas composition and a lower temperature were used. Some traces of ammonia are found in the absence of external hydrogen gas, as hydrogen atoms are also produced from water sonolysis.

Thermodynamic calculations suggest that some ammonia formation should occur in the "hot spot" with a temperature of about 5000 K believed to be present. The decrease of formation rate with T indicates that kinetics – not equilibrium – is the dominant consideration for synthesis of sonochemical ammonia.

The presence of ions in the solution has an opposite effect for ammonia formation. They decrease ammonia formation steadily with increasing time of sonication.

The ammonia can be produced in organic media, but the presence of a catalyst in this media seems it does not increase the rate of ammonia formation significantly. This is still the initial study for catalytically ammonia formation with ultrasonic irradiation. More studies about the effect of catalysts in the sonochemical formation of ammonia are needed.

Suggestion For Future Work

There are a number of questions raised by the results of this work. These questions can only be answered with more research. Some of them are described below:

6.1. Ammonia in Octane as a Function of Composition of Gas

The study of formation of ammonia in octane was done by using conditions that were used in water. At gas mol fraction of 0.6 nitrogen, the ammonia formation in octane was very small, approximately just 10% of that in water. Some direct experiments are needed on the variation of the rate of formation with gas composition of N_2/H_2 in octane. Such new work is also useful to derive a better understanding of the mechanism for sonochemical formation of ammonia, as some ammonia was formed in water with the absence of external hydrogen gas.

6.2. Ammonia with Different Catalysts

It is necessary to study in more detail possible catalytic effects on sonochemical formation of ammonia. One of the important properties of catalysts that are involved in a reaction is surface area. Thus, a further study for sonochemical formation of ammonia with different solid powder catalysts is required.

6.3. Ammonia at 20 kHz

The design of a reaction vessel for 20 kHz ultrasound in our lab is appropriate to maintain a circulation of powdered catalyst in the volume with greatest cavitation activity. However, it has not yet been proven that ammonia can be formed sonochemically with 20

kHz ultrasound. If it proves to be possible, then it opens up the possibility of simple experiments with a wide variety of possible catalyst.

6.4. Nitrate and Nitrite with Different Salts Present

The presence of ions (KCl) can increase the rate of total nitrate formation 10 fold; it also decreases the oxidation of nitrite to nitrate. A possible explanation of decreasing oxidation of nitrite is due to the reaction between chloride ions and hydroxyl radicals that eventually form hydrogen peroxide that oxidizes nitrite to nitrate. More investigations with different salts are needed to clarify these phenomena.

References

Anbar, M.; Pecht, I. **1964**, *J. Phys. Chem.*, **68**, 1460.

Anbar, M. **1968**, *Science*, 161, 1343.

Asquith, P.L.; Tyle, B.J. **1970**; *In*: Cotton and Wilkinson, *Advanced Inorganic Chemistry, a Comprehensive Text*, 3rd Edition, **1972**, John Wiley and Sons, New York.

Atkins P. **1998**, *Physical Chemistry*, 6th Ed., 68- 70.

Battino, R. **1981**; *In*: Fogg, P.G.T.; Gerrard, W., *Solubility of Gases in Liquids*, **1991**, John Wiley and Sons, New York.

Battino, et al. **1984**; *In*: Fogg, P.G.T.; Gerrard, W., *Solubility of Gases in Liquids*, **1991**, John Wiley and Sons, New York.

Byrne, J.E., et al. **1974**, *J. Chem. Thermodynamics*, 6, 245.

Currell, D.L.; Zechmeister, L. **1958**, *J. Am. Chem. Soc.*, 80, 205.

Didenko, et al. **1999**, *J. Am. Chem. Soc.*, 121, 5817-5818.

Sokol'skaya, A.V.; El'piner, I.E. **1957**; *In*: I.E. El'piner, *Ultrasound: Phys. Chem. and Biol. Effects*, **1964**, Consultans Brean, New York.

Entezari, M.H.; Kruus, P. **1994**, *Ultrason. Sonochem.*, 1, S75.

Entezari, M.H. **1994**, Ph.D. Thesis: *The Effect of Frequency on Sonochemical Reactions*, Carleton University, Canada.

Entezari, M.H.; Kruus, P.; Otson, R. **1997**, *Ultrason. Sonochem.*, 4, 49.

Faust, R., et al. **1999**, *Word records in Chemistry*, Wiley-VCH, New York, 75-127.

Fenkel, J. **1948**; *In*: Webster, E., *Ultrasonics*, **1963**, 1, 39-38.

Flint, E.B. **1991**; *In*: Didenko, et al., *J. Am. Chem. Soc.*, **1999**, 121, 5817-5818.

Fischer, Ch.H.; Hart, E.J.; Henglein, A. **1986**, *J Phys Chem.*, 90, 1954.

Fitzgerald, et al. **1954**, *J. Chem. Phys.*, 25(5), 926-933.

Fogg, P.G.T.; Gerrard, W. **1991**, *Solubility of Gases in Liquids*, John Wiley and Sons, New York.

Gaitan, D.F., et al. **1992**, *J. Acoust. Soc. Am.*, 91, 1373-1520.

Galloway, W.J. **1954**, *J. Acoustic, Soc. Am.*, 26, 848.

Green, M.; Sykes, A.G. **1970**, *J. Chem. Soc., A*, 3209.

Handbook of Chemistry and Physics, **1999**, 80th Ed., CRC Press LLC, New York.

Hart, E.J.; Henglein, A. **1985**, *J. Chem. Phys.*,89, 4342.

Hart, E.J.; Henglein, A. **1986**, *J Phys Chem.*, 90, 5992.

Hart, J.H.; Fisher, Ch-H.; Henglein, A. **1990**, *J. Phys. Chem.*, 94, 284.

Herzberg, G. **1950**, *Molecular Spectra and Molecular Structure I. Spectra of Diatonic Molecules*, 2nd ed., Van Nostrand, Princeton, New York.

Heywood, J.B. **1988**, *Internal Combustion Engine Fundamentals*, McGraw-Hill, New York.

Hueter, T.F. **1955**, *Sonics*, John Wiley and Sons, Inc., New York, 243, 83.

Huheey, J.E. **1978**, *Inorganic Chemistry: Principles of Structure and Reactivity*, Harper and Row Publishers, new York.

Jarman P.D. and Taylor K.J. **1965**, *J. Appl. Phys.* 16, 675.

Kruus, P. **1987**, *J. Phys. Chem.*, 91, 3041.

Kuttuff H. **1991**, *Ultrasonics*: Fundamental and Applications, Elsevier applied science, London, 377-384.

Lange's Handbook of Chemistry, **1979**, 12th ed , McGraw-Hill, New York.

Lauterbon, W., **1973**, *Proc. Symp. Finite-Amplitude Wave Effects in Fluids*, Copenhagen.

Lee, Y.N. *In: Gas-Liquid Chemistry of Natural waters*, Vol.1 BNL 51757 **1984** Brookhaven National laboratory, as quoted in: Seinfeld, J.H.; Pandis, S.N. *Atmospheric Chemistry and Physics* **1998**, John Wiley and Sons, New York.

Lewis G.N. and Randall M., **1923**, *In*: Raymond E. K., *Encyclopedia of Chemical Technology*, Volume 1, **1947**, The Interscience Incyclopedia, Inc., New York.

Libes S.M. **1992**, *An Introduction to marine biogeochemistry*, Joh Wiley and Son Inc., New York, 432-433.

Lindstrom, O. **1955**, *J. Acoust. Soc. Am.*, 27, 654.

Makranczy, J., et al. **1976**; *In*: Fogg, P.G.T.; Gerrard, W., *Solubility of Gases in Liquids*, **1991**, John Wiley and Sons, New York.

Margulis, M.A.; Didenko, Y.T. **1984**, *Russ. J. Phys. Chem.*, 5, **848**.

Mason, T.J. et al. **1994**, *J. Ultrason. Sonochemistry*, 1(2), S91-S95.

Mead, E.L.; Sutherland, R.G.; Verrall, R.E. **1976**, *Can J Chem.*, 54, 1114.

Mizukoshi, et al. **1999**, *Ultrason. Sonochemistry*, 6(4), 203-209.

Morita, M. **1966**, *Canadian Patent 732,592*, Method for Improving the Taste of Alcoholic Liquors.

Petrier, C.; Jiang, Y.; Francony, A.; Lemay, M.F. *In*: Nies, U. (eds.) *Technical University of Hamburg –Hamburg Reports on Sanitary Engineering* **25**: Ultrasound in Environmental Engineering (ISSN 0724-0738; ISBN 3-930400-23-5), **1999**, 167-180.

Plesset M.S. **1949**, Trans. ASME., *J. Appl. Mech.* 75, 277.

Rayleigh, L. **1917**; *In*: Suslick, K.S., *Ultrasound, its chemical, physical, and biological effect*, **1988**, VCH Publishers, Inc.

Renaudin, V, et al. **1994**, *J. Ultrason. Sonochemistry*, 1(2), S81-S85.

Riesz, P. et al. **1985**; *In*: *Petrier et al., J. Phys Chem* , **1994**, 98, 10514-10520.

Rodel S.R. and Navidi M. **1994**, *Chemistry*, 2nd Ed., West publishing Company, New York, 726-727.

Seinfeld, J.H.; Pandis, S.N. **1998**, *Atmospheric Chemistry and Physics*, John Wiley and Sons, New York.

Schultes, H.; Gohr, H. **1936**, *Angewandte Chemie*, 49, 420.

Shriver, D.F.; Atkins, P. **1999**, *Inorganic Chemistry*, 3rd Ed., W.H. Freeman and Company, New York.

Smith, F.D. **1935**; *In*: Crawford, A.E., *Ultrasonic Engineering*, **1955**, Butterworths Scientific Publications, London.

Sokol'skaya, A.V. **1978**, *J Gen Chem USSR*, 48, 1289.

Spinks J.W.T and Woods R.J., **1990**, *An Introduction to Radiation Chemistry*, 3rd Edition, Wiley, New York.

Suslick, K.S.; Cline Jr.; R.E.; Hammerton, D.A. **1986**, *J Am Chem Soc.*, 108, 1986.

Suslick, K.S.; Mdeleleni, M.M.; Ries, J.T. **1997**, *J Am Chem Soc.*, 119, 9303.

Suslick, K.S. **1988**. *Ultrasound, its chemical, physical, and biological effect*, VCH Publishers, Inc.

Suslick, K.S. **1990**, *American association for the advancement of science*, 247, 1520.

Thornycroft, J., Barnaby, S.W. **1895**; *In*: Suslick, K.S., *Ultrasound, its chemical, physical, and biological effect*, **1988**, VCH Publishers, Inc.

Tiehm, A. **1999**; *In*: Tiehm, A.; Nies, U (eds) *Technical University of Hamburg Reports on Sanitary Engineering 25: Ultrasound in Environmental Engineering* (ISSN 0724-0738; ISBN 3-930400-23-5), **1999**, 167-180.

Tremper, K.K.; Prausnitz, J.M. **1976**, *J. Chem. Eng. Data*, 21, 295.

Twigg M.V. **1996**, *Catalyst Handbook*, 2nd Ed., Manson publishing Ltd., p.25).

Virtanen, A.I.; Ellfolk, N. **1950**, *J Am Chem Soc*, 72, 1046.

Wakefold, C.A.; Blackburn, R.; Lickiss, P.D. **1999**, *Ultrason. Sonochem*istry, 6, 141.

Weast, R.C.(ed). **1967**, *Handbook of Chemistry and Physics*, 48th ed., The Chemical Rubber Co., Cleveland.

Webster, E. **1963**, *Ultrasonics*, 1, 39-38.

Weissler, A., et al. **1950**, *J. Am. Chem. Soc.*, 72, 1769.

Weissler, A. **1959**, *J. Am. Chem. Soc.*, 81, 1077.

Wilhelm, Solubility Data Series, Vol. 5/6, Hydrogen and Deuterium, ed. C.L. Young, Pergamon, Oxford, **1981**; *In*: Fogg, P.G.T.; Gerrard, W., *Solubility of Gases in Liquids*, **1991**, John Wiley and Sons, New York.

Yen T.F. **1999**, *Environmental Chemistry, Essentials of Chemistry for Engeneering practice*, Prentice Hall Inc., New Jersey, 321-323.

Appendix A.1

Calibration of the Rotameter

A Matheson gas rotameter or flow rate meter (Model 7630T-602) was used to determine the volumetric gas flow rates for mixtures of N_2/O_2 and N_2/H_2 with different compositions, but equal total flow rate, 2.90 mL s^{-1}. The calibration of this rotameter was carried out by passing the gases through the rotameter and then through the soap bubble flow meter. In this process a timer was used to record the time for different volumes of gases. The calibration was done at a temperature of 25 ($\pm$ 2) °C.

The calibration curves are presented in figures (A.1.1, A.1.2 and A.1.3). Note that they can not be used if the flow rate is too small. Each point represents the average of three runs.

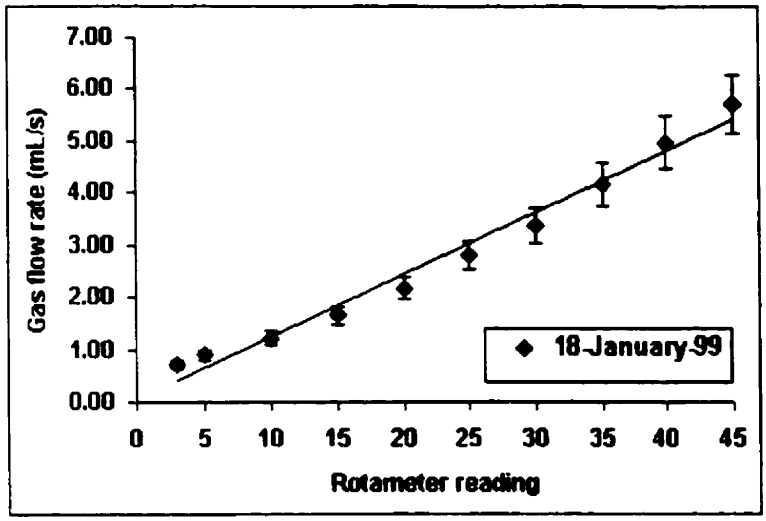

Figure(A.1.1): Calibration curve for the rotameter using N_2 gas at (25 ± 2)°C.

Equation:
F.rate = 0.0738 + 0.1182(Rot)

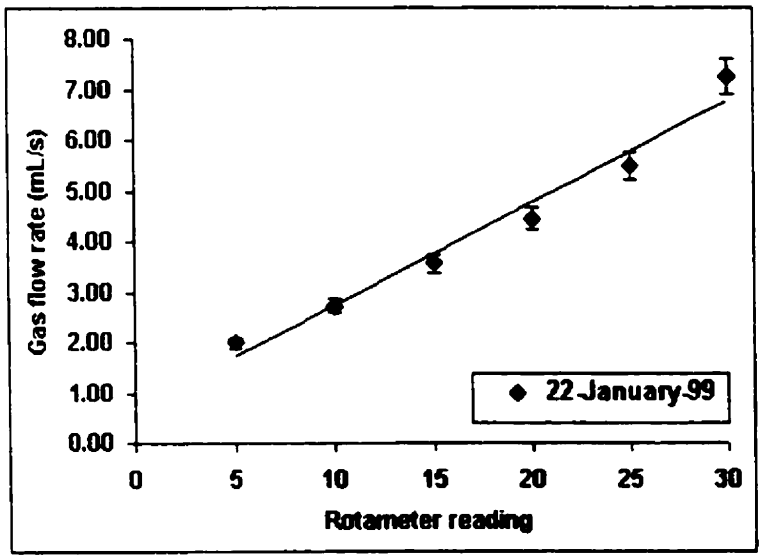

Figure(A.1.2): Calibration curve for the rotameter using H_2 gas at (25 ± 2)°C.

Equation:
F.rate = 0.6974 + 0.2026(Rot)

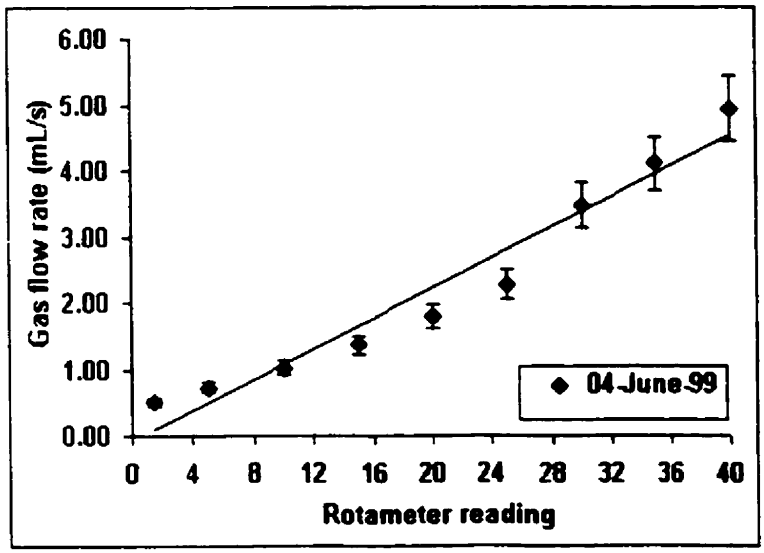

Figure(A.1.3): Calibration curve for the rotameter using O_2 gas at (25 ± 2)°C.

Equation:
F.rate = -0.0747 + 0.1149(Rot)

Appendix B.1

Calibration of the Nitrate Ion – Specific Electrode

Crystalline potassium nitrate (see section 3.1.1) was used to prepare a calibration curve for determination of the nitrate concentration of samples. This curve was made by measuring potentials (mV) of different concentrations of potassium nitrate solutions with a nitrate ion specific electrode (refer to section 3.2.1) and a single junction reference electrode (see section 3.2.1). In this process, 2.0 mL of ionic strength solution ($(NH_4)_2SO_4$, 2.0 M) was added to 100.0 mL of standard or sample nitrate solutions before measurement. The potential was recorded when its value had been constant for at least 3 minutes. The calibration was done at a temperature of 25 ($\pm$ 2)°C.

The potential readings for standard nitrate solutions are provided in tables (B.1.1). The calibration curves are presented in figures (B.1.1). Each point represents the average of three runs.

Table (B.1.1): Calibration data for standard nitrate solutions at (25 $\pm$ 2)° C.

Concentration (M)	Potential (mV)
4.00×10^{-5}	186.3 $\pm$ 7.1
8.00×10^{-5}	172.0 $\pm$ 5.7
2.00×10^{-4}	149.3 $\pm$ 5.1
4.78×10^{-4}	130.8 $\pm$ 2.4
5.96×10^{-4}	125.8 $\pm$ 3.1
9.91×10^{-4}	111.6 $\pm$ 2.2
1.96×10^{-3}	96.7 $\pm$ 2.2
3.85×10^{-3}	79.4 $\pm$ 2.6
5.66×10^{-3}	69.2 $\pm$ 1.3
7.41×10^{-3}	62.4 $\pm$ 1.2
9.97×10^{-3}	54.6 $\pm$ 1.5

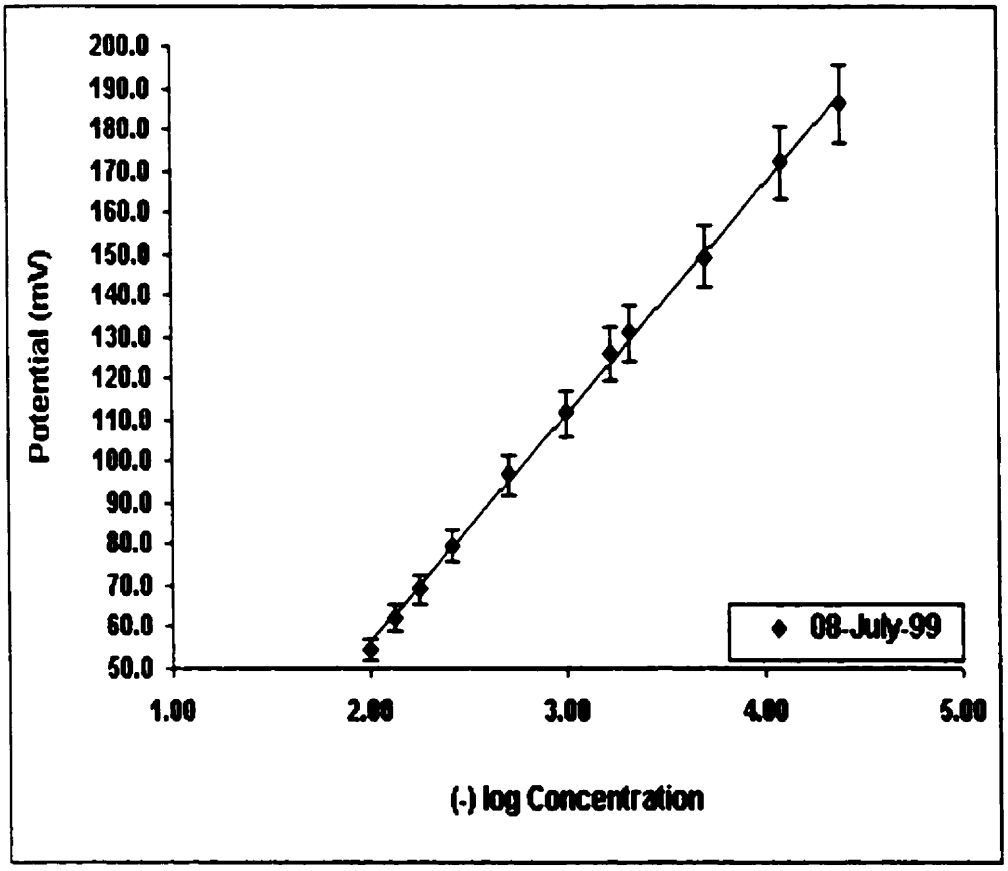

Figure B.1.1. Calibration curve for the (-)log standard nitrate concentration versus potential.

Equation: ***(-) log concentration = 0.984 + 0.018 (potential)***

Appendix B.2

Calibration of Nitrate in Ionic Strength Solutions

Crystalline potassium nitrate (see appendix B.1) dissolved in potassium chloride solution (see section 3.1.1) was used to prepare a calibration curve for determination of the nitrate concentration in samples in KCl solutions. This curve was made by measuring potentials (mV) of different these concentrations with a nitrate ion specific electrode and a single junction reference electrode (see appendix B.1). The potential was recorded when its value had been constant at least 3 minutes. The calibration was carried out at a temperature of 25($\pm$ 2)°C.

The calibration curves are presented in figures (B.2.1 and B.2.2). Each point represents the average of two runs.

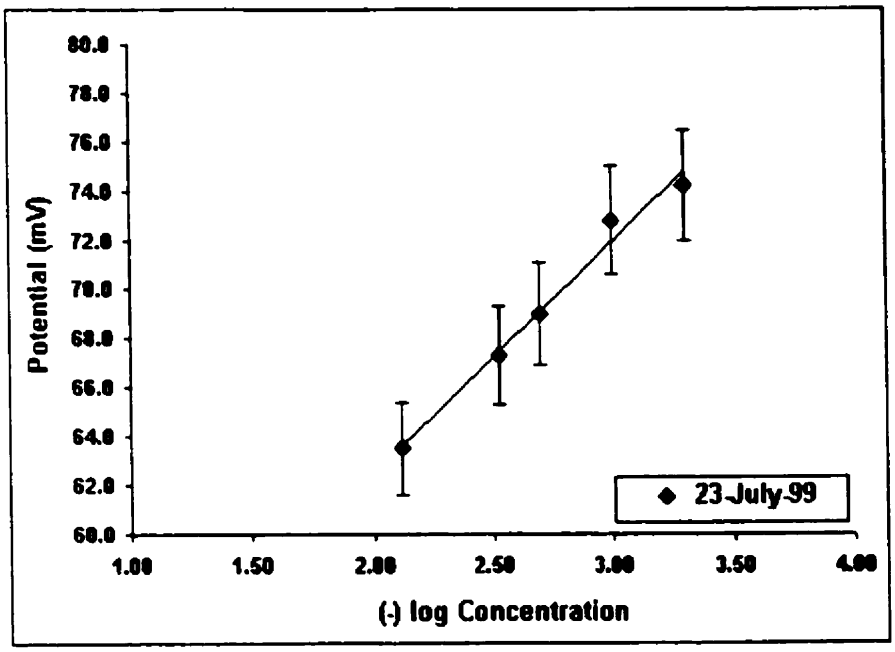

Figure B2.1. Calibration curve for the (-) log standard nitrate concentration in KCl (1.14M) versus potential

Equation: ***(-) log concentration = -4.496 + 0.104 (potential)***

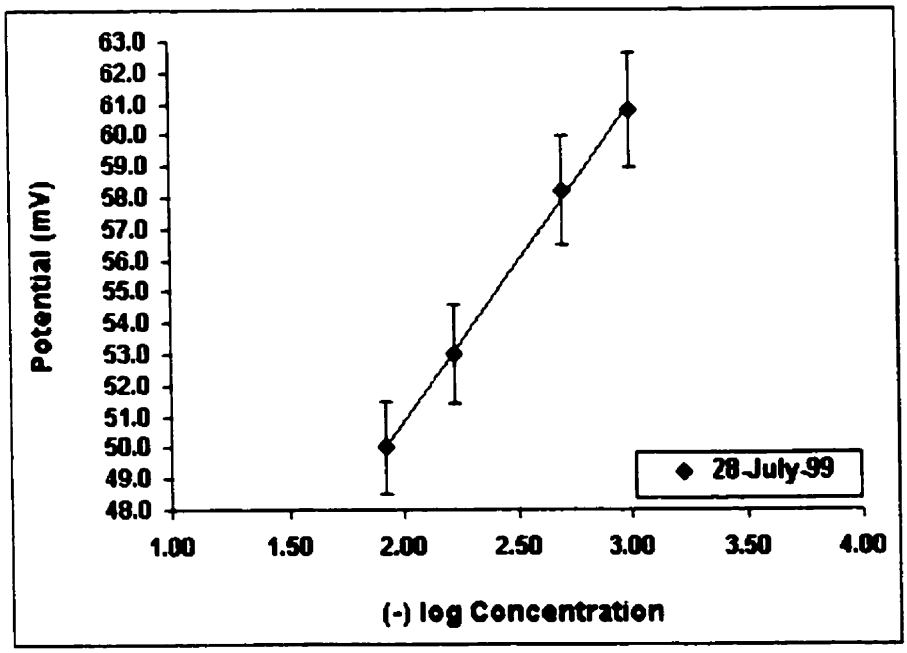

Figure B2.2. Calibration curve for the (-) log standard nitrate concentration in KCl (2.28M) versus potential

Equation: ***(-) log concentration = -3.001 + 0.098 (potential)***

Appendix B.3

Oxidation of the Nitrite Solutions to Nitrate with Hydrogen Peroxide

Hydrogen peroxide was used as an oxidant to convert nitrite to nitrate in sample solutions. The volume of hydrogen peroxide solution needed in this process was determined by oxidizing standard potassium nitrite solutions with it (refer to experimental for their purities). In this process, 100 mL samples of 2.00×10^{-4} M potassium nitrite were oxidized with different volumes of hydrogen peroxide solution. The residual hydrogen peroxide in the solutions was eliminated by boiling them at least 20 minutes on a hot plate, after stirring them overnight. The solutions were cooled to room temperature ($25(\pm 2)^{o}C$). Deionized water was then added to them until the volume was 100 mL. The potential of the nitrate ion specific electrode was then measured in the solutions after adding 2.0 mL of 2.00 M ammonium sulphate ionic strength solution (see B.1).

The potential readings for potassium nitrite solutions are provided in tables (B.3.1). The curves are presented in figures (B.3.1). Each point represents the average of two runs.

Table (B.3.1): Volume data of hydrogen peroxide solutions for oxidizing nitrite ions at (25 ± 2)°C.

Volume of H_2O_2 (mL)	(Nitrite) M	Potential (mV)	(Nitrate) M
1.0	2.00×10^{-4}	170.3	8.85×10^{-5}
2.0	2.00×10^{-4}	165.6	1.08×10^{-4}
5.0	2.00×10^{-4}	151.5	1.81×10^{-4}
10.0	2.00×10^{-4}	149.4	1.99×10^{-4}

Note: potential of 100mL KNO_3 (2.00×10^{-4} M) + 2 mL ISA (2.00 M) is 149.3 mV.

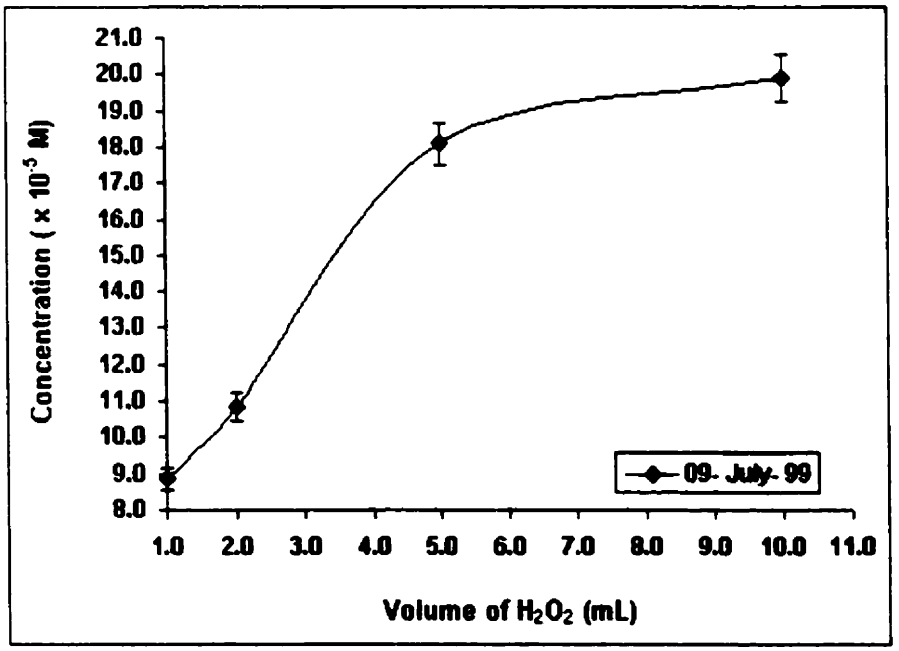

Figure B.3.1. Curve for the nitrate concentration from oxidation of potassium nitrite versus volume of H_2O_2.

Appendix C.1

Calculation of Ammonia Concentration from pH

Concentrations of ammonia obtained during sonication of a mixture of N_2 and H_2 gases were indirectly determined with a pH meter. The precise concentration of total ammonia is then calculated based on the equilibrium constant of ammonia. An example of these calculations is shown below:

	NH_3 + H_2O ========	NH_4^+ +	OH^-
Initial state:	a	0	0
Reaction:	$-x$	x	x
Equilb. State:	$(a-x)$	x	x

Equilibrium constant (K_b) = $(NH_4^+)(OH^-)/ (NH_3) = (x)^2/(a-x) = 1.79 \times 10^{-5}$ at 25°C.

Therefore total $(NH_3)_t = a = (x)^2 / 1.79 \times 10^{-5} + x$.

As an example, in one experiment, the initial pH of water (before sonication) was measured to be 6.26, or $-\log_{10}(OH^-) = pOH = 7.74$. The final pH of water (after sonication) was 9.31 or pOH = 4.69 at 23°C. Based on this equation, the initial (OH^-) can be ignored because the value is too small compared to the final (OH^-). Assuming that the K_b is constant in this small range of temperature and ionic strength, the concentration of total ammonia is thus

$(OH^-) = x = 10^{-pOH} = 10^{-4.69} = 2.04 \times 10^{-5}$ M

$(NH_3)_t = (x)^2 / 1.79 \times 10^{-5} + x$

$(NH_3)_t = [(2.04 \times 10^{-5})^2 / 1.79 \times 10^{-5} + 2.04 \times 10^{-5}]$ M = $(NH_3)_t = 4.37 \times 10^{-5}$ M.

A determination of ammonia by titration with HCl (2.3×10^{-4} M) was attempted. The titration was, however, unsuccessful due to reaction of CO_2 from the air with the

sample. Determinations with dilute strong acids would have to be carried out in a grove box in order to prevent exposure to normal air.

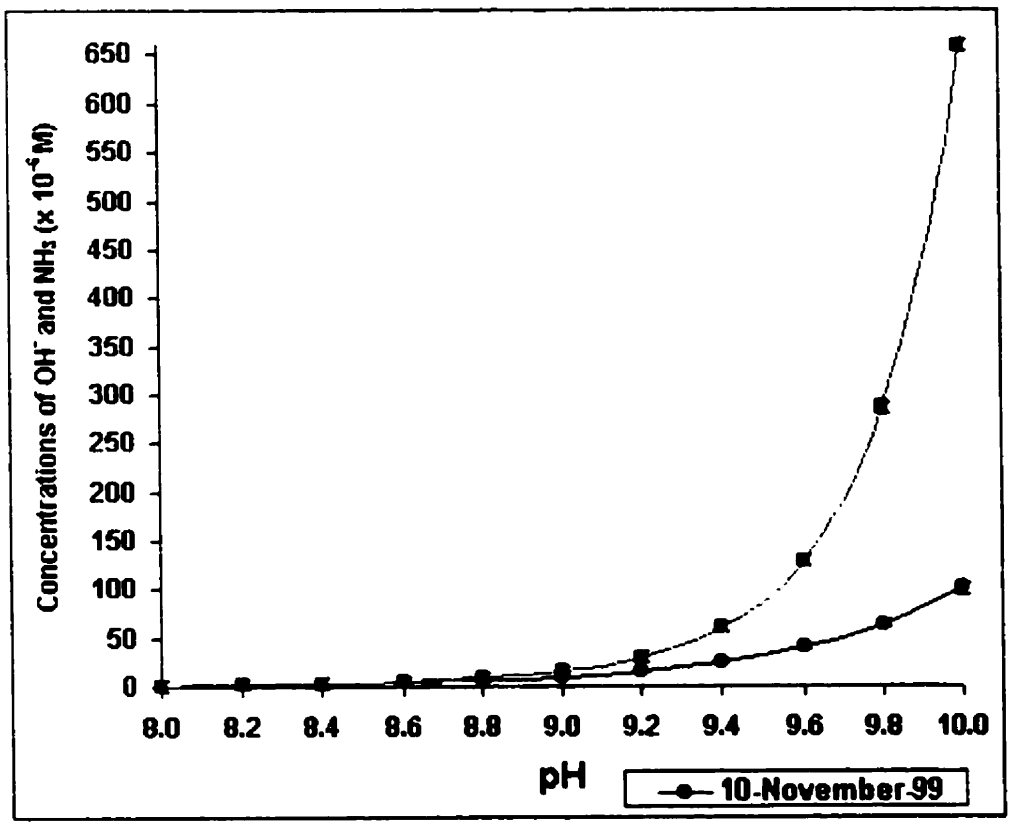

Figure C.1. Calculated curves for concentrations of hydrogen ions and ammonia versus the pH.

Appendix C.2

Calculation of Ammonia Concentration from pH in Ionic Strength Solutions

When a mixture of N_2 and H_2 was sonicated in a solution of KCl (1.0 M), the effect of ionic strength has to be accounted for in the calculation of concentration of ammonia based on pH. An example of the calculation is given below:

$$NH_3 + H_2O \equiv\equiv\equiv\equiv\equiv\equiv\equiv\equiv\equiv NH_4^+ + OH^-$$

$K = a(NH_4^+)a(OH^-) / a(NH_3) = 1.79 \times 10^{-5}$, at 25°C, where $a = {}_\gamma c$.

$K_w = a(OH^-)a(H^+) = 1.0 \times 10^{-14}$

$c(NH_4^+) + c(H^+) = c(OH^-)$ (Electric neutrality)

Here a, γ, and c refer to an activity, activity coefficient and concentration respectively.

Experimental data: The pH in KCl (1.0 M) was 9.41 after sonication, and γ for KCl (1.0 M) is 0.657 (HCP, 1998).

Assuming $\gamma = 0.657 = {}_\gamma(NH_4^+) = {}_\gamma(OH^-) = {}_\gamma(H^+)$, the calculation of total concentration of NH_3 is as follow:

$pH = -\log_{10} a(H^+) = 9.41$, thus $c(H^+) = 10^{-9.41} / 0.657 = 5.92 \times 10^{-10}$ M.

$a(OH^-) = 1.0 \times 10^{-14} / 10^{-9.41} = 10^{-4.59}$, and $c(OH^-) = 10^{-4.59} / 0.657 = 3.91 \times 10^{-5}$ M.

Thus $c(NH_4^+) = 3.91 \times 10^{-5} - 5.92 \times 10^{-10} = 3.91 \times 10^{-5}$ M.

$c(NH_3) = a(NH_3) = a(NH_4^+)a(OH^-)/ K = (3.91 \times 10^{-5} \times 0.657)^2 / 1.79 \times 10^{-5} = 3.69 \times 10^{-5}$ M.

$c(NH_3)_{tot} = (3.69 \times 10^{-5} + 3.91 \times 10^{-5})$ M $= 7.60 \times 10^{-5}$ M.

Appendix D.1

Calibration of Standard NH_4Cl with Nessler'Reagent

Crystalline ammonium chloride (see section 3.1.1) was used to prepare a calibration curve for determination of the ammonia concentration of samples. This curve was made by measuring absorbance of different concentrations of ammonium chloride solutions with Perkin-Elmer Lambda 4B UV/VIS spectrophotometer at a wave length of 396 nm with 10.0 mL of HCl (1.0×10^{-5} M) added by 0.05 mL of Nessler'reagent as a blank solution. In this process, 0.05 mL of Nessler'reagent was added to 10.0 mL of standard or acidic sample ammonium solutions before measurement. The calibration was carried out at a temperature of $25 \pm (2)^{o}C$.

The absorbance readings for ammonium chloride solutions are provided in tables (D.1). The calibration curve is presented in figure (D.1).

Table (D.1) Calibration data for standard ammonium chloride solution at $25 \pm (2)^{o}C$.

Concentration ($\times 10^{-6}$M)	Absorbance
0.5	0.178 ± 0.0018
1.0	0.180 ± 0.0030
10.0	0.226 ± 0.0115
50.0	0.477 ± 0.0010
100.0	0.790 ± 0.0212

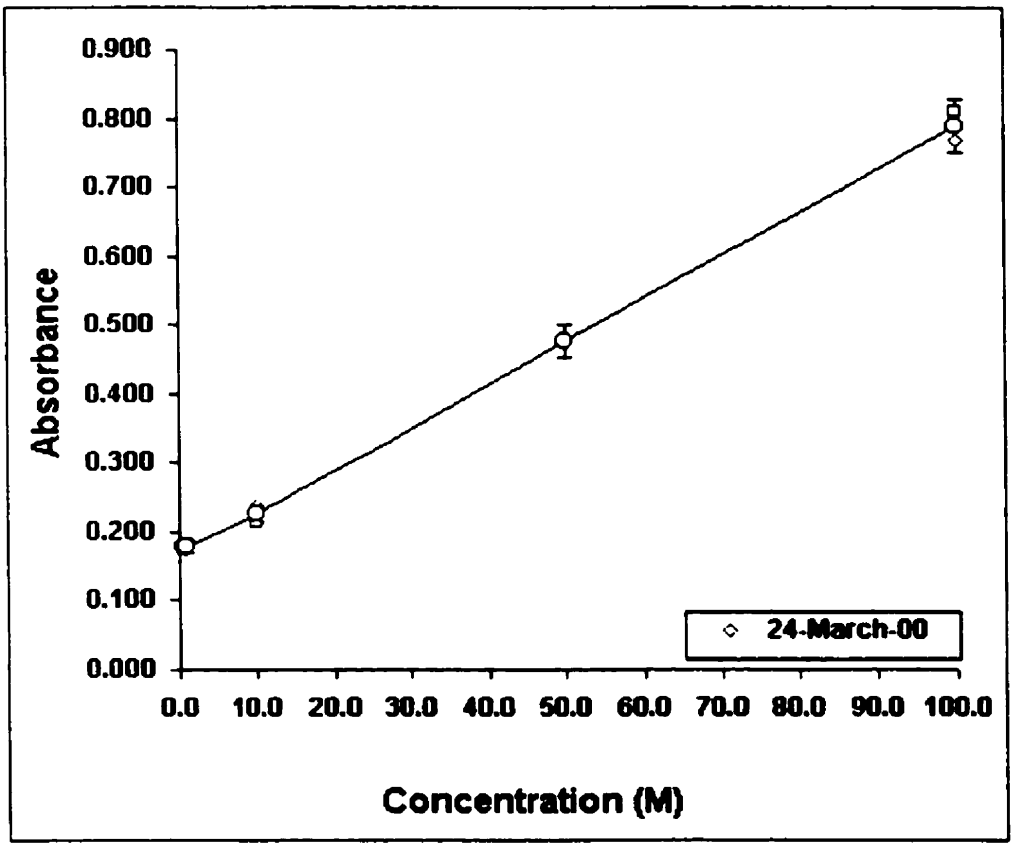

Figure D.1. Calibration curve for standard ammonium chloride solutions versus absorbance.

Appendix E.1

Calibration of Iodine in KI Solutions

Crystalline iodine and potassium iodide (see experimental) were used to prepare a calibration curve for determination of the iodine concentration of samples. This curve was made by measuring absorbance of different concentrations of iodine in KI (0.20 M) with a Spectronic 21 visible spectrometer at a wave length of 355 nm with KI (0.20) M as a blank solution. The calibration was carried out at a temperature of 25 $\pm$ (2)°C.

The absorbance readings for iodine solutions are provided in tables (E.1). The calibration curve is presented in figure (E.1). Each point represents the average of three runs.

Table (E.1) Calibration data for standard iodine in KI (0.20 M) solution at 25 $\pm$ (2)°C.

Concentration (M)	Absorbance
0.000000	0.000 $\pm$ 0.000
1.00×10^{-6}	0.103 $\pm$ 0.0015
3.00×10^{-6}	0.323 $\pm$ 0.0006
5.00×10^{-6}	0.513 $\pm$ 0.0010
8.00×10^{-6}	0.859 $\pm$ 0.006

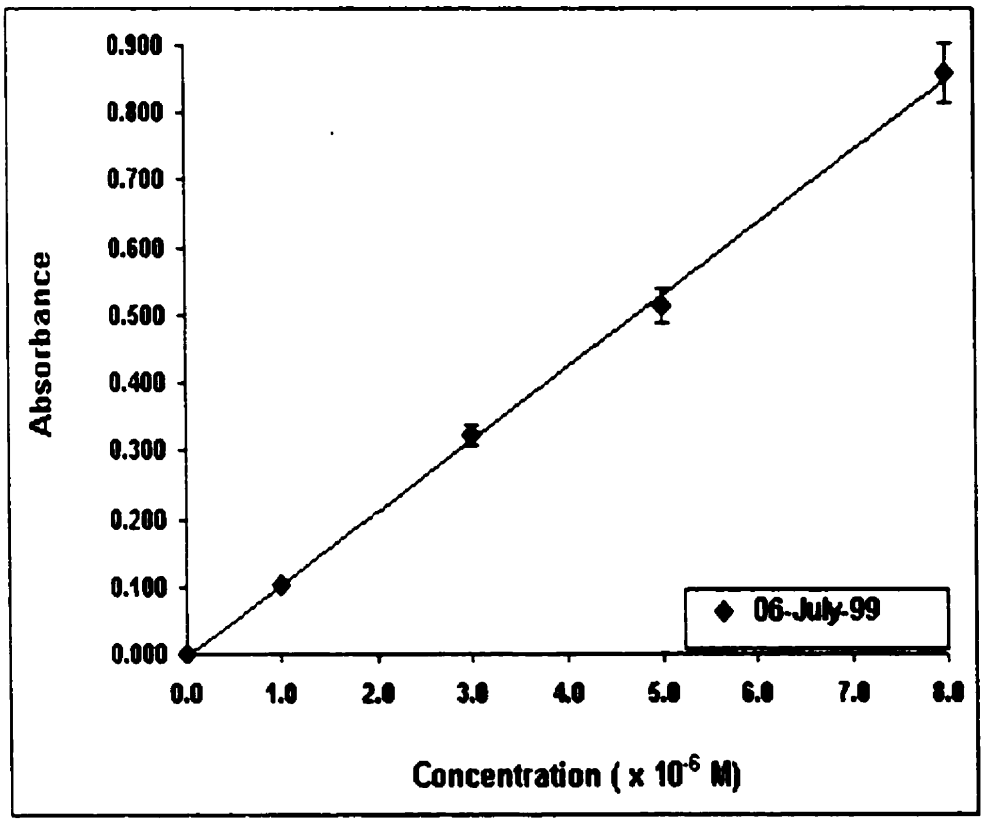

Figure E.1. Calibration curve for standard iodine solution in KI (0.20 M) versus absorbance. Equation: ***Absorbance = -0.003 + 0.107 (concentration)***.

Appendix E.2

Calibration of the Calorimetric Method for Determining Ultrasonic Power

A calorimetric method was used to determine the power of the ultrasonic reactor. The temperature of a 100 mL sample of deionized water was measured as function of time in a reactor cell at 30 second intervals. This was done both with the power on and off. The power was then calculated with the equation below:

$$\text{Power} = m.Cp(dT/dt) = m.Cp[(dT/dt)_{on} + (dT/dt)_{off}]$$

Here the unit of power in Watt = $J\ s^{-1}$; mass = m in kg; heat capacity = Cp in $J\ kg^{-1}K^{-1}$; absolute temperature = T in Kelvin (K) and time = t in second (s). This was done in order to eliminate the effect of heat loss from the reactor.

Based on these above, the power of a 900 kHz reactor with a frequency of 971 kHz was 27 Watt. This is equivalent to formation on 15.14 μ mol iodine in 20 minutes (see E.1).

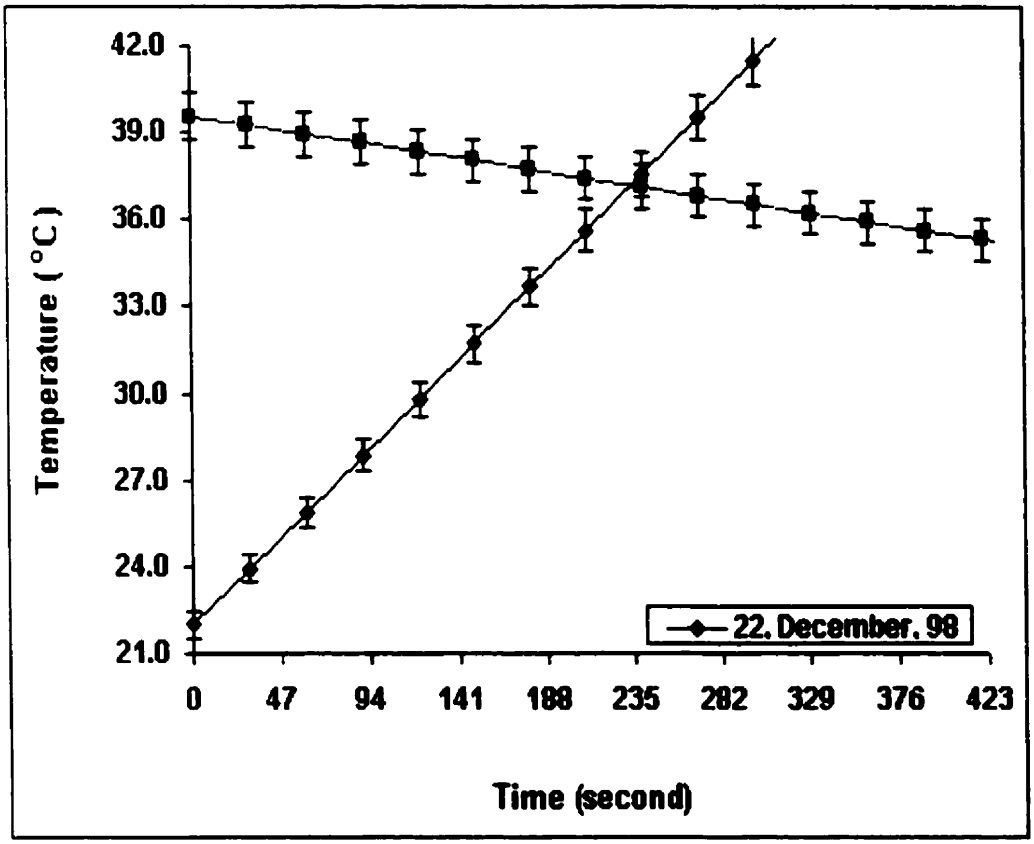

Figure E.2. Calibration curve of the calorimetric method for 900 kHz ultrasonic with frequency 971 kHz.